Global and Planetary Change 195 (2020) 103321

Contents lists available at ScienceDirect

Global and Planetary Change

journal homepage: www.elsevier.com/locate/gloplacha

Facies and implications of a coarse-grained lacustrine onshore paleo-tsunamiite: An integrated study of an upper Miocene bouldery cobble gravel

Orsolya Sztanó[a,*], Soma Budai[a], Imre Magyar[b], Gábor Csillag[c,1,2], Judit Nadrai[a], László Fodor[a,d]

[a] Department of Geology, Eötvös Loránd University, Pázmány Péter sétány 1/C, 1117 Budapest, Hungary
[b] MTA-MTM-ELTE Research Group for Paleontology, POB 137, 1431 Budapest, Hungary
[c] Geological and Geophysical Institute of Hungary, Stefánia út 14, 1143 Budapest, Hungary
[d] MTA-ELTE Geological, Geophysical and Space Science Research Group, Pázmány Péter sétány 1/C, H-1117 Budapest, Hungary

ARTICLE INFO

Keywords:
Boulder
Lacustrine
Paleo-tsunami deposit
Paleo-seismicity
Slope collapse
Extreme wave event

ABSTRACT

Gravelly tsunami event beds are well known from some contemporary shores, but they are far less known from the pre-Quaternary depositional record. Lacustrine examples are particularly exceptional. Here we present multidisciplinary evidence for a lacustrine cobble to boulder gravel deposited as an onshore paleo-tsunamiite and discuss features that help to identify the depositional setting. The deposit was formed on the rocky shore of a large peninsula within the late Miocene Lake Pannon (Hungary). The lake was several hundred meters deep, and near to the study area it was about 50–80 km wide. The inferred paleo-tsunami deposit includes subangular clasts that are exclusively derived from the underlying Cretaceous sandstone. Imbrication of the bouldery gravel points to landward transport of the clasts, however, a 15-cm-thick lens of cross-bedded sand records an opposing flow direction. The clayey sand matrix contains fossils, i.e. fragmented and articulated mollusc shells, as well as ostracods, that lived on the nearby sandy shoreface and offshore. The facies of the gravel indicates a short-distance transport of clasts typical for an extreme wave event. None of the depositional features e.g. various degree of clast roundness, seaward dipping imbrication, bidirectional transport indicators, clast-supported fabric, large thickness of beds, and lack of grading is either unique to tsunami deposits or excludes storm wave origin. An extreme storm wave origin, however, is discarded in this case, when paleogeography and climate are considered. The combination of matrix-supported fabric, presence of a mixed clayey-sandy matrix in the clast-supported parts, and preservation of articulated mollusc shells, as well as mixture of clasts and fossils from different zones of the shore, identify these beds as paleo-tsunami deposits. As coeval volcanism is not known, a hypothetic tsunami could have been related either to an earthquake along nearby normal faults or to large-scale sliding events on the closely located shelf slope due to rapid deposition or seismic shocks. The recognition of these event beds reinforces structural observations on the syn-depositional character of nearby faults, active after the middle Miocene climax of synrift tectonics in the Pannonian Basin. Thick, boulder-sized onshore paleo-tsunamiites are useful indicators of a paleogeographic situation in which tsunami waves were amplified to produce noticeable beds in the rock record.

1. Introduction

Tsunamiites (sensu Shiki and Yamazaki, 2008) occur worldwide along many modern coastlines, but their facies varies greatly from fossiliferous mudstones to boulder fields and their locations range from offshore to onshore. Most of the recent tsunami-related deposits can be directly linked to historically recorded events, such as large earthquakes, volcanic eruptions and/or related submarine slides. The research interest of tsunami-related depositional processes and deposits largely increased after the 2004 and 2011 well known events from the Indian and Pacific Oceans (Costa and Andrade, 2020). In addition to these recent occurrences (e.g. Matsumoto et al., 2010; Goto et al., 2012, Chagué-Goff et al., 2011; Etienne et al., 2011; Goto et al., 2014), a large number of modern examples is known from the Atlantic and

* Corresponding author.
E-mail addresses: sztano@caesar.elte.hu (O. Sztanó), budai.soma@gmail.com (S. Budai), immagyar@mol.hu (I. Magyar), gabor.csillag.53@gmail.com (G. Csillag), lasz.fodor@yahoo.com (L. Fodor).
[1] MTA-ELTE Geological, Geophysical and Space Science Research Group, Pázmány Péter sétány 1/C, H-1117 Budapest, Hungary.
[2] Research Centre for Astronomy and Earth Sciences, Institute for Geological and Geochemical Research, Budaörsi út 45, H-1112, Budapest, Hungary.

https://doi.org/10.1016/j.gloplacha.2020.103321
Received 29 March 2020; Received in revised form 20 August 2020; Accepted 9 September 2020
Available online 14 September 2020

Mediterranean regions of Europe (Dawson et al., 2004; Kortekaas and Dawson, 2007; Costa et al., 2011; Scicchitano et al., 2007; Dawson et al., 2019), New Zealand (Goff et al., 2001), Japan (Richmond et al., 2012; Goto et al., 2015; Pilarczyk et al., 2019), around oceanic volcanic islands (Moore and Moore, 1984; Pérez-Torrado et al., 2006; Paris et al., 2017), Chile (Abad et al., 2020) or the Cascadian margin (Peters et al., 2007). Most of the above examples are subaerially exposed onshore tsunamiites, commonly referred to as tsunami deposits (Shiki and Yamazaki, 2008), which have a limited preservation potential, except for the very coarse-grained ones (Dawson and Stewart, 2007; Goto et al., 2014).

Fine-grained tsunami deposits are typically composed of sand (Gelfenbaum and Jaffe, 2003; Morton et al., 2007; Bahlburg et al., 2018; Goto et al., 2019) and commonly found as anomalously coarse layers between deposits of low energy coastal marshes and ponds (Peters et al., 2007; Matsumoto et al., 2010). Coarse-grained deposits can be represented by distinct boulders (Etienne and Paris, 2010, Goto et al., 2012), boulder fields (Mastronuzzi et al., 2007; Maouche et al., 2009; Etienne et al., 2011; Erdmann et al., 2017; Hoffmeister et al., 2020) and gravel (Moore, 2000; Pérez-Torrado et al., 2006; Morton et al., 2008; Paris et al., 2011, 2018), in nearshore or backshore regions.

The study of modern onshore tsunamiites yielded a list of criteria, including their sedimentary facies, composition and bedding, ecology of redeposited fauna, which can be useful for the identification of tsunami deposits either generated by undetermined triggering events or described from the geological past (Goff et al., 2012). However, none of these features nor their combination was found to indicate unambiguously a tsunamigenic origin, because most of these are shared with other extreme waves events such as major storms (Goff et al., 2001, Felton et al., 2006; Kortekaas and Dawson, 2007; Morton et al., 2008; Goto et al., 2014, 2015; Costa and Andrade, 2020; for a comprehensive list of arguments see Shanmugam, 2012). Other attributes, such as original elevation above the water level, onshore distance from the shoreline, or morphology of the shore are not known sufficiently accurate even in cases of pre-historical, yet Holocene tsunamis. The same holds for dimensions of the water body (i.e. areal extent, paleo-water depth) that help to reconstruct the mode of deposition, or numerical modeling of tsunami waves (cf. Dawson et al., 2019). In other cases, modeling of boulder transport either by tsunami or storm waves (Costa et al., 2011; Dewey and Ryan, 2017; Lario et al., 2020; Hoffmeister et al., 2020) requires specification of parameters not available for ancient examples. Subsequent erosion, which is common in any coastal setting from storm-wave base to the subaerially exposed backshore, may also remove evidence of deposition by tsunami waves. Incomplete records and/or other uncertainties about the paleo-conditions could lead to arbitrary interpretations and discussions about paleo-tsunami and storm deposits (cf. Scheffers et al., 2005; Morton et al., 2008; Erdmann et al., 2017; Dewey and Ryan, 2017), or paleo-tsunami and fault-related alluvial deposits (Cantalamessa and Di Celma, 2005; Bahlburg et al., 2010), or paleo-tsunami and rocky shoreface deposits (Moore and Moore, 1984; Felton et al., 2006) among others. Although an increasing number of studies have described pre-Holocene paleo-tsunamiites (e.g. Bourgeois et al., 1988; Shiki and Yamazaki, 1996; Fujino et al., 2006; Wang et al., 2015; Jarochowska and Munnecke, 2015; Slootman et al., 2016; Dewey and Ryan, 2017), examples of modern and few thousand-year-old cases are still far more numerous than descriptions of older ones. Further in the deep-time rock record for which circumstances are more speculative, identification of paleo-tsunami deposits and distinction from other extreme wave events are challenging and still based mainly on the facies of the deposit. This highlights the importance of well-established pre-Holocene examples.

Triggering mechanisms of (paleo-)seismic events, including earthquakes, under-water slides, or volcanic eruptions, can undoubtedly operate not only in marine systems near plate margins, but also in lakes in the interior of continents, and thus are able to induce tsunami waves (e.g., Ichinose et al., 2000; Dawson and Stewart, 2007; Törő and Pratt, 2016; Falvard et al., 2018). Nonetheless only several examples of lacustrine tsunamiites have been reported so far from intracontinental areas. These include large mass transport deposits from Alpine lakes, where correlation between volume of mass slides and height of tsunami wave was established (Schnellmann et al., 2006; Hilbe and Anselmetti, 2014; Kremer et al., 2015). Other lacustrine examples are mud-clast and/or peat-clast bearing sand beds in coastal lakes of Chile and Portugal (Kempf et al., 2017; Costa et al., 2012) and products of the Storegga Slide along the coastal lakes of Norway (Bondevik et al., 1997; Vasskog et al., 2013). These latter lakes are important archives of paleo-tsunami deposits with a higher preservation potential than that of subaerially exposed parts of coastal plains (Kempf et al., 2017), however, they are controlled by processes generated in the nearby marine system and not by the lacustrine ones.

Here we describe an example of a cobble to boulder gravel which we infer to be an onshore paleo-tsunamiite from the late Miocene Lake Pannon, Central Europe, which was not under any marine influence. The paleogeography of the lake is fairly well-constrained (Magyar et al., 2013; Sztanó et al., 2016), as well as the climate of this period (Böhme et al., 2008), therefore extreme wave events of storm origin are very unlikely to have occurred. Independent evidence for roughly coeval earthquakes and/or major slope collapse events providing triggering mechanism is available (Fodor et al., 2013). Our objective is to demonstrate that a combination of sedimentary features and paleontological characteristics could be considered helpful to identify paleo-tsunami deposits in the rock record. We show this is possible even though many features of paleo-tsunami deposits are shared by gravelly onshore storm deposits, such as coarse-clast shoreface ridges or cliff-top gravels. This study promotes recognition of a yet underestimated sort of paleo-event bed in the sedimentary archives. It highlights the significance of paleo-tsunami deposits as valuable indicators of paleo-seismicity, regardless of their lacustrine or marine depositional setting.

2. Geological setting

The upper Miocene gravel discussed herein is located in the Gerecse Hills at the junction of the northern segment of the Transdanubian Range and the Kisalföld–Danube Basin of the Pannonian Basin System (Fig. 1a). The Pannonian Basin is a result of lithospheric extension within the Alpine–Carpathian orogenic belt (Royden and Horváth, 1988; Balázs et al., 2016). Extension started at around 18.5 Ma and the syn-rift deformation was accompanied by neutral to felsic volcanism (Harangi and Lenkey, 2007), partly related to subduction below the orogenic arc. Major episodes of volcanism occurred between 17 and 14 Ma within the Pannonian Basin (Lukács et al., 2018), although magmatism continued up to recent times in the Eastern Carpathians (Seghedi et al., 2011). Syn-rift faulting resulted in the formation of several major half grabens (Csontos, 1995), the Kisalföld–Danube Basin being one of them (Tari, 1994; Kováč et al., 2006); the elevated edge of this large-scale asymmetric graben is represented by the NE–SW trending Transdanubian Range. Although syn-rift faulting ceased around 15 Ma in the western Pannonian Basin, a renewal of faulting in the early late Miocene was documented all along the Transdanubian Range (Fodor et al., 2013; Magyar et al., 2017), possibly due to reorganization of major blocks, mantle dynamics and subduction geometry between ca. 12–9 Ma (Balázs et al., 2017a).

Post-rift sedimentary fill of the Kisalföld–Danube Basin started at 11.6 Ma (Šujan et al., 2016). At that time the vast (ca. 240,000 km^2 area), up to 1000 m deep, brackish Lake Pannon occupied the entire Pannonian Basin (Magyar et al., 1999; Balázs et al., 2018). The

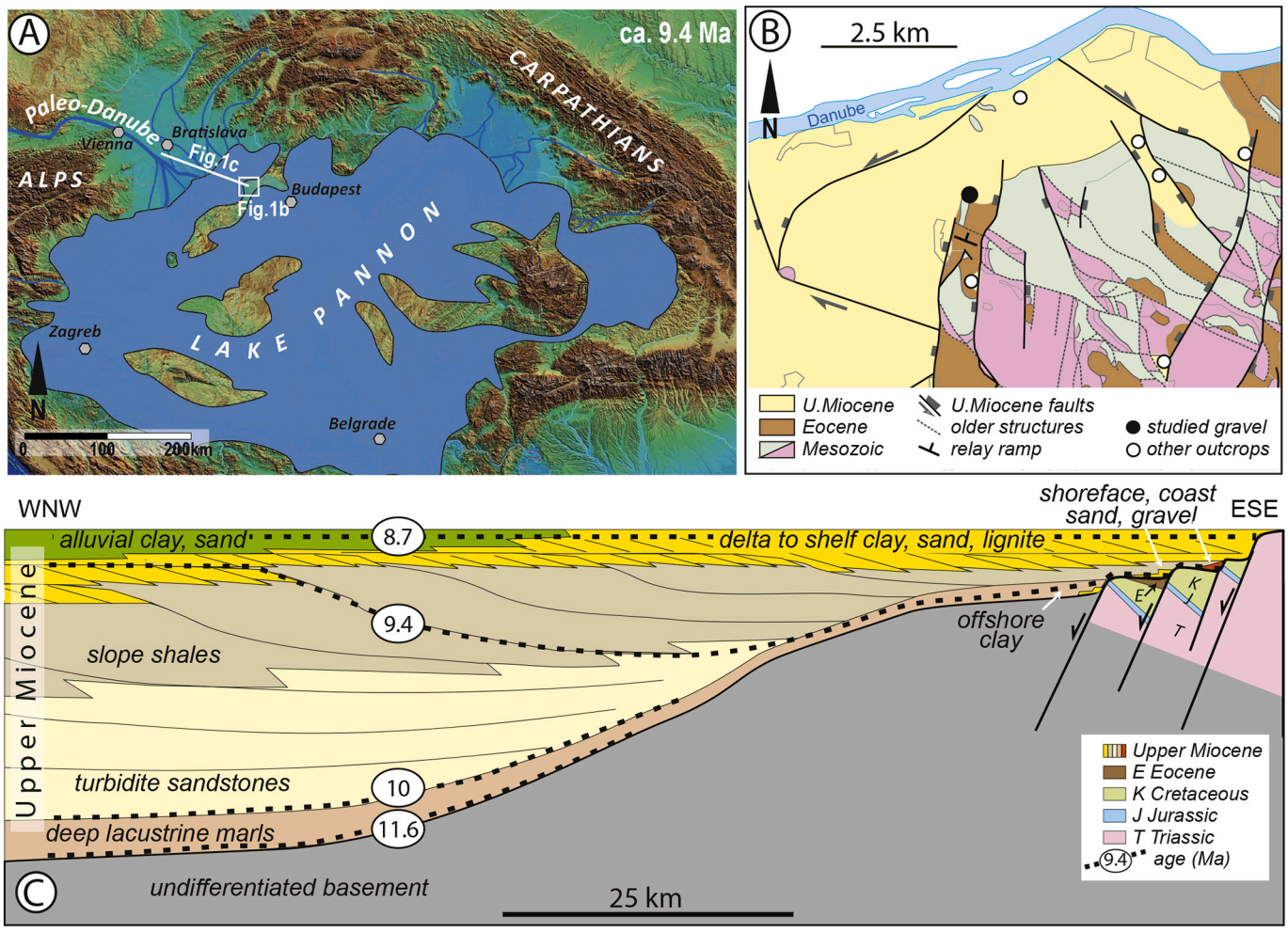

Fig. 1. A) Lake Pannon at about 9.4 Ma in central Europe with location of the study area indicated. B) Simplified geological map of the area, modified after Fodor et al., 2013. C) Geological cross-section representing the conditions at about 8.7 Ma from the Kisalföld—Danube Basin (KDB) to the marginal successions at the Transdanubian Range (TR) study site (modified from Sztanó et al., 2016).

Transdanubian Range, as one of the basement highs of the complex lake bottom, partially separated the Kisalföld–Danube Basin from the rest of the lake, forming a large gulf (Fig. 1a; Sztanó et al., 2013a, 2016). Sedimentation started with deep-water mudstones and turbidites and continued from ca. 10 Ma onwards with rapid NW-to-SE progradation of a ca. 550 m high shelf-margin slope (Magyar et al., 2013; Sztanó et al., 2016; Balázs et al., 2018). The accretion of the shelf was fed by deltaic to alluvial systems arriving from the Alpine–West Carpathian orogenic belt. On the northwestern, shallow flanks of the Transdanubian Range, however, deposition of the lacustrine sedimentary succession (Fig. 1a) started much later with a flooding event, dated at 9.4–9.2 Ma by bio- and magnetostratigraphy (Cziczer et al., 2009; Magyar et al., 2013, 2017; Magyar, 2020). Here, the succession is made up of locally sourced fossiliferous shoreface sand, which partly interfingered and later was overlain by lacustrine offshore clay. This clay was deposited at an estimated water depth of up to 80 m (Cziczer et al., 2009), and made a relatively shallow, wide and flat margin connecting the deep basin interior and the coast (Fig. 1c). Both sandy and rocky coasts were located on the edge of the Transdanubian Range (Sztanó et al., 2016; Magyar et al., 2017). Based on mollusc biostratigraphy (Magyar et al., 2017), the upper Miocene bouldery cobble gravel described herein is coeval with the sandy shoreface deposits, the offshore clay, and the shelf-edge slope deposits prograding from the NW (Fig. 1b). At this time the lake between the peninsula and the northwestern deltaic shorelines was only about 50–80 km wide, and the basin was closed from the northeast, where different nearshore sediments deposited (Kováč et al., 2006). Flooding of the coast of the Transdanubian Range was followed by the complete infilling of the Kisalföld–Danube Basin, thus deltas reached the study area less than 1 million years after the initial flooding (Magyar et al., 2017). On the long-term flooding, determined by lithospheric processes (Balázs et al., 2017a), short-term climate-driven lake-level changes with an amplitude of 20–30 m were superimposed (Sztanó et al., 2013b; Balázs et al., 2017b).

The late Miocene climate of the Pannonian basin was warm temperate. Based on the botanical and palynological record, the mean annual temperature (MAT) is estimated between 13 and 16 °C, with frostless winters and less than 20 °C annual range (Nagy, 2005; Hably, 2013). Estimates of the mean annual precipitation (MAP), based on botanical and mammal records, scatter between the extreme values of 1950 and 354 mm, and often involve a temporal trend (e.g. Böhme et al., 2008; Kovar-Eder and Hably, 2006). The MAP values most probably remained within the realistic interval of 700–1300 mm, with a clear maximum at about 9.7–9.2 Ma. The „Vallesian crisis", i.e. the sudden decrease of diversity in land mammals, especially the forest-dwelling ones after ca. 9.5 Ma, during deposition of the studied

Fig. 2. A) Exposure of a late Miocene fault plane just south of the study site. B) The fault breccia and C) the Miocene pebbles are composed of the Triassic limestone of the foot wall (modified from Fodor et al., 2013).

sediments, is well constrained in the Pannonian basin (Nargowalla et al., 2006). The crisis is interpreted as a consequence of increasing aridity and seasonality, a phenomenon characteristic for mid-latitudinal lands worldwide.

There are several lines of evidence for syn-sedimentary fault activity along the western margin of the Transdanubian Range, including its northern part, which was bounded mostly by normal faults (Fig. 1b, c; Fodor et al., 2013; Sipos-Benkő et al., 2014). Direct indications, such as tectonic breccias in the hanging wall of the western boundary fault (Fig. 2), are testament to structural activity during the flooding (Fodor et al., 2013; Fodor et al., 2018). At the same location locally-derived, well-rounded, well-sorted carbonate pebbles of abrasional origin (Fig. 2) may indicate a fault-controlled lake margin, only 1.5 km distance from the coeval bouldery gravel, discussed herein. Between two overlapping fault segments, a northward tilted relay ramp is documented, which sharply deviated deltaic distributary channels during regression less than a million years later (Fig. 1b, Bartha et al., 2015; Fodor et al., 2018). The investigated site is located on the relay ramp (Fig. 1b). These data indicate that fault activity, albeit possibly episodic, was ongoing during the entire time span of the sedimentation.

The upper Miocene gravel, which is the focus of the present study, was deposited on an irregular erosional boundary with the Cretaceous sandstone (Fig. 3). Clasts are exclusively made up of the underlying sandstone, the sediment is poorly sorted and contains subangular cobbles to boulders. The Cretaceous sandstone beds were locally exposed and originally could have been situated at the ancient lakeshore. Elsewhere the Cretaceous sandstone is overlain by by Eocene mudstone (Fig. 1).

3. Results

3.1. Sedimentary facies

The upper Miocene bouldery cobble gravel is exposed in small stratigraphic thickness (up to 3.5 m) provided by a single natural outcrop along a creek (47° 42′ 54.90715″ N; 18° 23′ 33.378635″ E; Figs. 3, 4). It has an irregular, erosional contact with the underlying Cretaceous sandstone, and is unconformably overlain by Quaternary slope deposits. The Cretaceous sandstone beds are either very hard due to carbonate cementation or friable due to varying clay content.

The studied succession consists of a lower (ca. 1.25 m thick) and an upper (up to 2.5 m thick) gravel bed, separated by an irregular, yet poorly defined surface of meter-scale relief. A 20 cm thick, 1.5 m wide, lenticular sand body also occurs between them. The lower bed is a matrix-supported cobble gravel with pebble-boulder clusters (Fig. 4a, d). The matrix of the gravel is composed of clayey, poorly sorted, fine- to coarse-grained sand (Figs. 3; 4f). Fragmentary and well-preserved gastropod and bivalve (both articulated and disarticulated) shells of up to a few cm in size and ostracod valves are abundant in the matrix (Fig. 4d, e). Neither normal nor inverse grading is present. The upper bed is dominantly clast-supported (Figs. 3, 4), with considerably less muddy and sandy matrix. Fossils are very rare in the upper layer and grading or textural sorting is absent. The sand lens between the two gravel beds is composed of cross-bedded, coarse-grained sand that lacks any pebbles, but contains granule-sized shell hash. Foresets dip towards north, i.e., lakeward direction.

The grain size of the two gravel beds is similar except for the matrix. The size of the grains ranges from pebbles to boulders with an a-axis

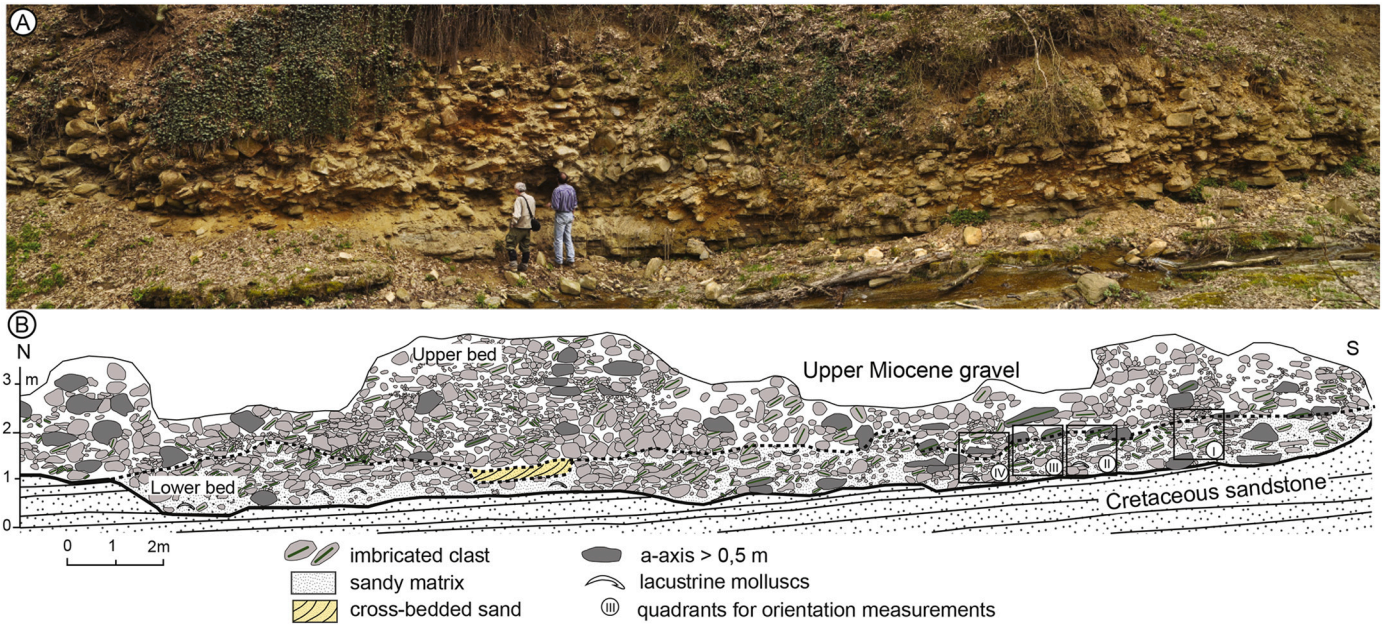

Fig. 3. A) Photomosaic of the studied outcrop and B) its line drawing interpretation. Note the bedding, clast imbrication, location of the largest boulders and the unconformity with the underlying sandstone. The cross-bedded sand lens is in the center covered by the geologists. Quadrants where imbrication was measured are also indicated (for close-up see Fig. 6).

exceeding 50 cm diameter; these boulders are scattered randomly (Fig. 3). All gravel-sized clasts but the mollusc shells are derived exclusively from the Cretaceous substratum, yet their roundness, sphericity and shape vary to a great extent. The majority of the clasts are of the hard type of sandstone, the friable ones are concentrated near the base (Fig. 4c).

Cobbles, which are the dominant size class (ca. 70% of the counted clasts; Fig. 5), are predominantly rounded blades (ca. 50%), but discoidal and elongate cobbles are also common (each ca. 20%). Pebbles, on the other hand, are mostly well-rounded discs or spheroids. Most of the boulders, however, are angular to sub-angular with slightly rounded edges, and have a blade- or disc shape, which is inherited from the abrasion pattern of the parent rock. Bed thickness in the Cretaceous substratum is up to 25 cm, which limited the size of boulders at least along one axis and affected the possible axial proportion of the clasts.

Clast shape, dimensions of the three axes, and for non-equant clasts dip-direction and -angle of 155 clasts (i.e. a-axis or ab-plane depending on shape) were measured in four 1 m^2 area quadrants in the lower bed (Fig. 6a). The a-axis and ab-plane of clasts are commonly imbricated in both beds (Fig. 3). Range of dip directions is related to grain size, deviation is smaller in boulders, but gets larger with the decrease of grain size (Fig. 6c). The NW–NE oriented dip direction of the imbricated clasts reveals transport towards SE–SW (Fig. 6e).

3.2. Fossils

The sandy matrix contains fossils of bivalves, gastropods, and ostracods (Fig. 4d, e). The identified forms all represent the highly endemic brackish-water biota of Lake Pannon. Among the bivalves, two dreissenid species are abundant: *Congeria* aff. *simulans turgida* and *Dreissenomya (Sinucongeria) arcuata*. The first species is widely distributed in the northwestern foreland of the Transdanubian Range. It lived on the sandy substratum of the littoral zone, often in large colonies (Szilaj et al., 1999; Magyar et al., 2017). In contrast, *D. arcuata* is known only from a few localities in the Pannonian Basin, typically from littoral sands. As a sinupalliate bivalve, it is considered to have lived an infaunal life. It was a shallow burrower into soft sediment (Marinescu, 1977; Harzhauser and Mandic, 2010). Shells of *D. arcuata* are found in large numbers in the matrix of the lower gravel bed, almost always with articulated valves. Due to subsequent dissolution, many specimens of the two dreissenid species lost their shell material and are preserved as internal moulds („steinkerns"). In addition to dreissenids, there are two species of Lymnocardiinae: a fragile fragment of *Paradacna* sp., and a few umbonal fragments of *Lymnocardium proximum*. The thin-shelled *Paradacna* was mostly (but not exclusively) a deep-water dweller, whereas L. *proximum* was a littoral species. Their shells were broken into angular pieces before being buried by the sediment.

The gastropods are represented by a few juvenile specimens of *Viviparus* sp. and a single specimen of *Melanopsis defensa*. Although shells of the typically freshwater *Viviparus* do occur together with brackish molluscs in the outcrops of littoral sands of Lake Pannon, they were typically abundant in freshwater environments of the delta plain, such as channels, ponds, and swamps, where they were accompanied by similarly freshwater snails and unionid bivalves. *M. defensa*, however, is a brackish-water littoral species, commonly associated with cardiids (Gillet and Marinescu, 1971; Magyar et al., 2017). Its single specimen from the outcrop is eroded and worn, indicating a longer-term abrasion before burial.

The ostracod fauna of the outcrop is also of low diversity: *Amplocypris* sp. and *Candona (Caspiolla)* sp. were identified. The latter is most common in shallow brackish waters, whereas *Amplocypris* most commonly (but not exclusively) lived in deeper water, below the wave base (e.g. Cziczer et al., 2009; Olteanu, 2011).

4. Discussion of depositional processes and environment

4.1. Origin of clasts: From abrasion to onshore mixing

The pebbles, cobbles and boulders were derived exclusively from erosion of the local Cretaceous sandstone substratum. Their monomict composition combined with different shape, size and roughness reveal various temporal exposure to reworking, i.e., to abrasional processes. The well-rounded, spherical pebbles and bladed cobbles point to repetitive wave action and they could have been rounded on the beachface. Gravel beaches, however, are typically built up by texturally-sorted, erosion-bounded, roughly parallel superimposed beds (e.g.

Fig. 4. Detailed sedimentary features of the gravel shown in Fig. 3. A) Grain composition and variously rounded clasts. Arrows show rip-up clasts derived from the uppermost silty sandstone bed of the underlying Cretaceous sandstone. B) Close up of the Cretaceous/Miocene unconformity. C) Rip-up siltstone clasts (arrows). D) and E) Intact and broken shells between coarse-grained sand, pebbles and cobbles. F) The matrix-supported lower and clast-supported upper beds. G) Close-up of the cross-bedded sand lens.

Massari and Parea, 1988; Postma and Nemec, 1990; Hayes et al., 2010; Lario et al., 2020). In contrast, the studied poorly-sorted, thick beds with an irregular base indicate that shaping and deposition of clasts occurred at different locations. Coexistence of different clast sizes with various shapes is also characteristic of gravel beaches. The subangular boulders and cobbles are interpreted to show only episodic abrasion, which probably took place during repeated storm events.

The a-axis imbrication of the elongated clasts in accord with the presence of the muddy matrix reveals a mass-flow type transport parallel to the a-axis, whereas ab-plane imbrication of discoid clasts marks only the direction of the shear stress and the transport (Davies and Walker, 1974; Nemec and Steel, 1984; Major, 1998). Taking into consideration the paleogeography of the area, a-axis and ab-plane imbrication reveals landward transport during deposition of the gravel, whereas the cross-bedded sand lens between the gravel beds points to lakeward transport.

The studied gravel represents a mixture of material originated from four different zones: 1) offshore (clay, *Amplocypris, Paradacna*), 2) shoreface (sand, *Congeria, Dreissenomya* (*Sinucongeria), Melanopsis*), 3) abrasional terraces (rounded pebbles – cobbles) and 4) the base of rocky cliffs (subangular boulders). This indicates that the clasts and shells, probably including living molluscs, were entrained, mixed, transported and deposited by an extreme wave event, i.e. either a tsunami or a major storm striking the onshore region. Now let's explore the characteristics of either type and their deposits in order to evaluate the likelihood of their activity.

4.2. Signatures indicating storm origin in gravelly onshore deposits

Storm waves are capable of powerfully reshaping beach faces, generate erosional surfaces and deposit clasts above high-water level (e.g. cobble-boulder armors, gravel to boulder ridges, ridge complexes, washover sheets, etc.; e.g. Hayes et al., 2010; Erdmann et al., 2017; Lario et al., 2020). The largest storms (hurricanes, typhoons) in oceanic settings are capable to overturn, pluck and transport boulders of up to several tens of tons weight far into the land or onto cliff tops several 10s m high (Williams and Hall, 2004; Goto et al., 2012; Erdmann et al., 2017; Dewey and Ryan, 2017; Hoffmeister et al., 2020). Although the

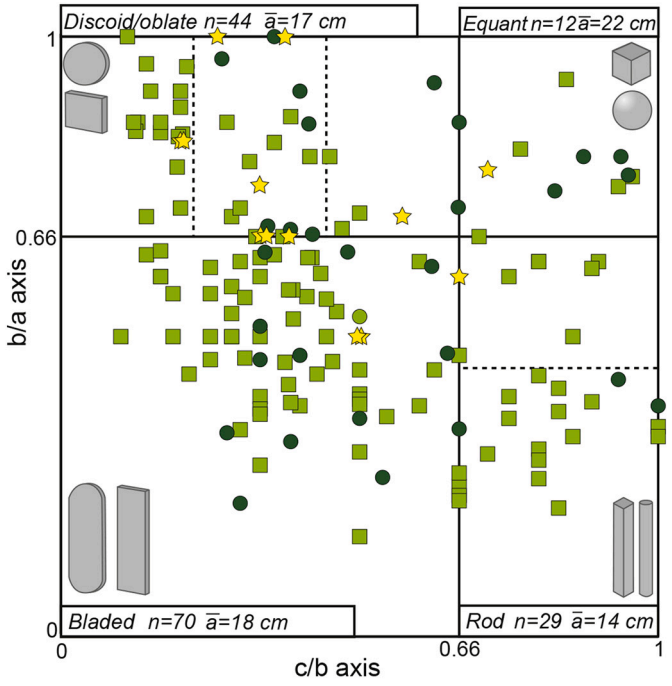

	Bladed	Rod	Discoid	Equant	Σ
Pebble	2	1	9	1	13
Cobble	55	25	27	5	112
Boulder	13	3	8	6	30
Σ	70	29	44	12	155

Fig. 5. Grain size and shape distribution of 155 measured clasts in the classification scheme of Zingg (1935) from selected quadrants. The number of clasts (n) and the average length of a-axis (ā) is indicated for each cluster. Slightly elongated, moderately flat cobbles are the most common clast type, probably reflecting the stratification and bed thickness of the parent Cretaceous sandstone.

grain size ranges from pebble to boulder in these deposits, the absence of mud is characteristic, as it does not settle from agitated water before waning of storm waves (Hall et al., 2006; Scheffers and Scheffers, 2006; Morton et al., 2008; Cox et al., 2012). Onshore storm gravels are often composed of multiple, moderately to well sorted layers of different clast sizes and shapes, arranged primarily by swash of high-energy waves, due to multiple events over centuries to millennia (Morton et al., 2008; Scheffers et al., 2009: Spiske and Halley, 2014). In such storm-related deposits clast-supported fabric is dominant (Hall et al., 2006; Cox et al., 2012). Open-framework is very common in modern deposits, but the interstices could also be filled by sand, which infiltrated later, e.g., either during the waning phase of the storm or long after, during other inundation events (Hall et al., 2006; Morton et al., 2008).

Prevalent waves during fair-weather conditions or storms generate seaward-dipping clast imbrication of discoidal pebbles, but shore-parallel orientation of the elongated ones was also reported (Williams and Hall, 2004; Hall et al., 2006; Morton et al., 2008; Hayes et al., 2010; Shanmugam, 2012; Spiske and Halley, 2014, Erdmann et al., 2017; Dewey and Ryan, 2017; Lario et al., 2020).

Finally, within beach gravels, mollusc shells, corals or other fragile macrofossils could be not only fragmented but edge-rounded with abrasion surfaces (Davies et al., 1989) primarily due to traction and collision due to fair-weather agitation. Storms mostly winnow and redeposit these biogenic clasts (Morton et al., 2008), moreover storms are not capable of eroding and redepositing shells from deep, distal zones of the shoreface (Kortekaas and Dawson, 2007; Donato et al., 2008).

The studied upper Miocene gravel is similar to the above described onshore storm deposits from many points of view, including the rounding of clasts, lake-ward dipping imbrication, clast-supported fabric of the upper bed and presence of fractured shells. Other features, like the lack of clear bedding, the poor sorting, the matrix-supported character of the lower bed, and the presence of the clayey-sandy matrix do not exclude a storm origin, but their coexistence is not supporting it either. The a-axis imbrication and the presence of articulated shells, the exhumation and transport of infauna of the lower shoreface are not typical for storm gravels.

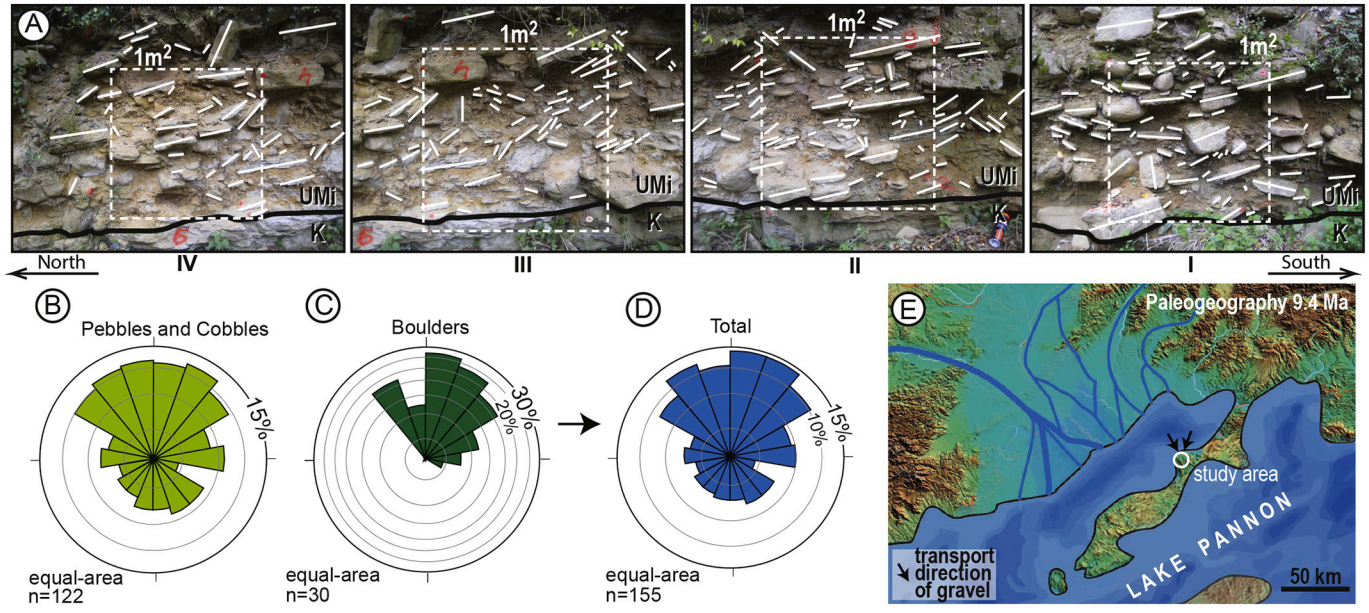

Fig. 6. Directional data of large clasts. A) The 1 × 1 m² quadrants where the measurement was carried out with an indication of a-axis or ab-plane imbrication as white lines. Rose diagrams of a-axis or ab-plane dip directions for B) pebbles and cobbles, C) boulders and D) all measured clasts. All indicate transport direction of gravel to the south. E) Paleogeography of Lake Pannon at the Kisalföld–Danube Basin, with the feeder river systems on the NW and the Transdanubian Penninsula on the SE side. Landward transport directions in the study area are displayed.

4.3. Signatures indicating tsunami origin in gravelly onshore deposits

The depth of erosion for a long-wavelength tsunami wave exceeds that of storm waves (Goto et al., 2014; Dewey and Ryan, 2017), therefore even a single tsunami wave could be capable of eroding and transporting small to very large clasts that originated from offshore to the backshore. The relatively short duration of the tsunami event, however, limits sorting and mixing of grain sizes from clay to boulders, in cases resulting in poorly-sorted deposits (Moore et al., 1994; Scheffers et al., 2005; Goff et al., 2012; Paris et al., 2013). One of the most important indicators of tsunami deposits could be the presence of mud in the matrix (Morton et al., 2007; Abad et al., 2020), while several different factors may result in its absence, thus careful consideration is needed. The amplitude and period of tsunami waves also influence transport processes. Tsunami waves reaching the shore commonly produce turbulent flows (Nanayama and Shigeno, 2006; Nanayama, 2008), but hyper-concentrated flows (Mulder and Alexander, 2001) or debris flows with large volume of suspension may also develop by erosion and entrapping of sand to clay from the nearshore area (Pérez-Torrado et al., 2006; Morton et al., 2007; Nanayama, 2008; Costa et al., 2011; Abad et al., 2020). The ratio of fine- to coarse-grained clasts determines whether matrix- (Nanayama and Shigeno, 2006) or clast-supported gravel with some matrix is deposited (Shiki and Yamazaki, 1996; Tanner and Calvari, 2004). Open framework fabric may point to original lack of fine-grained matrix or its removal by the back flow. Transport processes also determine whether normal, inverse or lack of grading develops in the deposit (Moore and Moore, 1984; Nanayama and Shigeno, 2006; Pérez-Torrado et al., 2006; Paris et al., 2011; Goff et al., 2012; Goto et al., 2019). Lack of grading mostly develops in gravels due to the short duration of transport followed by rapid deposition (Morton et al., 2007). Normally graded sand is very common and rather points to local tsunamis, while inverse grading may indicate regionally significant, large earthquakes (Goff et al., 2012).

In contrast to numerous waves during storms, a tsunami hits the coast in the form of a single wave or a few waves, resulting in clear phases of inundation and backwash (Dawson, 1994; Pérez-Torrado et al., 2006; Nanayama and Shigeno, 2006; Morton et al., 2007). These phases can be deduced from deposition of several beds and imbrication of clasts dipping seaward and landward, respectively, in subsequent beds (Nanayama et al., 2000; Fujino et al., 2006; Nanayama and Shigeno, 2006; Pérez-Torrado et al., 2006). Other paleo-current indicators, such as cross-bedding or cross-lamination may also be produced (Moore and Moore, 1984; Nanayama et al., 2000; Morton et al., 2007; Slootman et al., 2018; Paris et al., 2018). Backwash could be powerful enough to erode and transport talus or fluvial gravel from the inundated area back to the coastal region (Goto et al., 2019). It also can transport part of the sediment, swept previously onshore, back towards the main water body. The transport direction and capacity of the back flow highly depends on the topographic gradient and relief, and usually it follows local lows and may merge to scour channels or accelerate to supercritical flows near the beach (Morton et al., 2007; Slootman et al., 2018).

A wide variety of fossils occurs in many sorts of onshore tsunamiites, due to the erosional power of tsunami waves, which mobilize sediment of the sublittoral and littoral zones. As a result, fossil content of tsunami deposits commonly represents a mixture of taxa that lived in different habitats, at various water depths, and having distinct substrate-preferences (e.g. Moore and Moore, 1984; Fujino et al., 2006). Usually none of the remains are in life position except for boring bivalves, which were transported within boulders (Massari et al., 2009; Costa et al., 2011). The preservation of macrofossils, e.g. shells, varies from poor to perfect, depending on two factors: the pre-tsunami abrasion of disarticulated ones by wave agitation, and the matrix/clast ratio of the transporting tsunami, which when high, effectively prevents grain collisions and breaking of shells (Fujino et al., 2006; Pérez-Torrado et al., 2006; Donato et al., 2008; Massari et al., 2009; Paris et al., 2011, Puga-Bernabéu and Aguirre, 2017). Articulated shells were probably transported when they were still alive (Morton et al., 2008, Massari et al., 2009; Goff et al., 2012).

The studied upper Miocene gravel shares several features with onshore cobble to boulder tsunami deposits. The most important of these are the mixture of clasts and fossils from a wide range of coastal zones, the clayey-sandy matrix and the matrix-supported fabric together with a-axis type imbrication, all indicating landward transport in suspension as a mass flow. In several case studies the articulated shells were reported as indicators of erosion, short-term transport and rapid burial by tsunami events, thus the presence of such fossils could be an evidence for tsunami deposits. A potential backwash deposit is also present in the studied gravel deposits. Not only the bidirectional transport, but also the small number of beds and the rough erosional relief are in favor of the tsunami origin. None of the observed features opposes this interpretation.

4.4. Role of climate

Formation of storm waves capable of plucking and emplacing boulders in a lake is a function of local climate. Late Miocene paleontological climate proxies from the region reveal warm temperate conditions with a mean annual temperature of about 13-16 °C and a mean annual precipitation of 700–1300 mm (Böhme et al., 2008), slightly warmer and more humid than today. During and after the Vallesian crisis, when diversity of forest-dwelling land mammals decreased suddenly, aridity and seasonality might have increased in the Pannonian region (Nargowalla et al., 2006). Modeling of the modern climate of the region shows that increasing aridity during the last decades resulted in decreasing wind speed (Spinoni et al., 2015). Obviously, the paleontological data cannot be used as a proxy for late Miocene storm intensity or maximum wind speed. The regional wind direction might have been similarly from NW, though the topographic effect of the Alps and Carpathians was probably smaller. These winds thus might have crossed the 50–80 km wide Lake Pannon (Fig. 6), intensified wave force and contributed to the abrasional processes of the coasts facing to NW. At present, wind speed above 15 m/s (moderate gale) near ground level is very rare within the Carpathian area (Bartholy et al., 2003). That value is far too small to induce several meter high waves (e.g. exceeding 2–3 m) which are common in open marine settings and are capable of plucking and transporting 0.5 m-diameter boulders (e.g. Erdmann et al., 2017; Cox et al., 2018; Dewey and Ryan, 2017; Lario et al., 2020). In addition, model calculations demonstrated that a storm wave four times higher than a tsunami wave is required to transport a boulder of a certain mass (Cox et al., 2018; Dewey and Ryan, 2017; Hoffmeister et al., 2020). Therefore, violent storm events, which could have been capable of producing more than a meter-thick bed of bouldery gravel onshore, possibly in cliff-top position, are not likely to have occurred in the late Miocene Lake Pannon.

4.5. The inferred tsunami event in Lake Pannon

The studied gravel deposit is interpreted as the product of an extreme wave event, most likely as an onshore paleo-tsunamiite based on the sedimentary facies and fossil remains together with considerations of paleogeography and climate. The two gravel layers most likely represent the impact of two tsunami waves. Minutes could have elapsed between successive waves (cf. Dawson and Stewart, 2007; Morton et al., 2007; Dewey and Ryan, 2017). It is supposed that the first wave eroded and transported a mixture of pebbles, cobbles, boulders and high amount of sand and clay together with shells from different zones of the coast (Fig. 7a). The a-axis or ab-plane imbrication excludes rolling, the high proportion of matrix points to a rapid, cohesive debris-flow type surge, which resulted in deposition of the thick, poorly sorted, matrix-supported lower bed (Fig. 7b). After maximum inundation and stagnation was reached, a backwash current transporting mostly sand

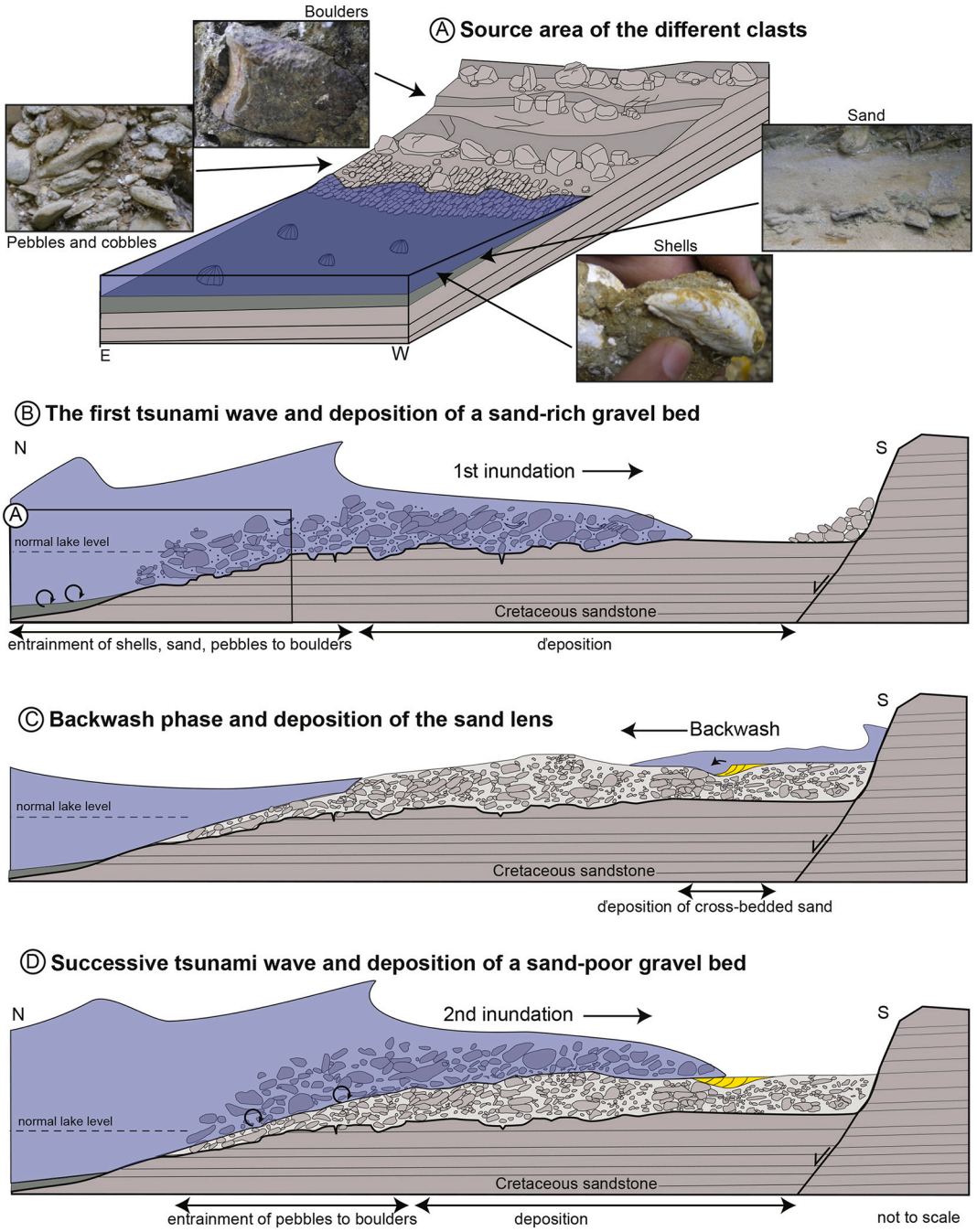

Fig. 7. Depositional model of the tsunami deposits. A) Source area of different grain classes, shapes and shells from offshore to backshore cliff-top. B) The first tsunami wave entraining and transporting the available material, from clay to boulders. C) Small sand dune depositing during backwash on top of the matrix-rich lower layer of the gravel. D) Formation of the upper layer by the second tsunami wave, probably transporting less sand.

developed, and small sandy dunes formed on the irregular surface of the gravel deposited during the inundation phase (Fig. 7c; cf. Nanayama et al., 2000). Imbrication pointing to lakeward transport was not recorded in the gravel beds. Absence of coarse material in the backwash sediment thus indicates relatively low-strength back flow and lack of funneling and acceleration, which commonly occurs in low relief coastal plains or far from the original coast (cf. Slootman et al., 2018). The precise extent of inundation cannot be constrained, but the Triassic carbonate bedrock, cropping out in a distance of 0.5–1 km, was not reached (Fig. 1), as reflected by the monomict composition of the gravel (i.e. lack of Triassic carbonate clasts), that may reveal localized inundation of a valley or a low lying coastal area (cf. Kortekaas and Dawson, 2007; Morton et al., 2007; Goto eat al. 2012; Goto et al., 2019).

For the deposition of the upper gravel bed, which has a clast-supported fabric and contains a much lower proportion of clayey-sandy matrix and shells, several scenarios are possible. Hence the tsunamigenic origin of the upper bed cannot be unequivocally demonstrated. Although the upper layer is thicker than the lower one, potential evidence of subsequent waves was not preserved and therefore it cannot be determined with certainty how many tsunami waves might have occurred. It is still most likely that it was produced by the second tsunami wave, eroding and transporting a smaller amount of fine-grained sediment from the shoreface (Fig. 7d), unless the sand was partly removed by the backflow.

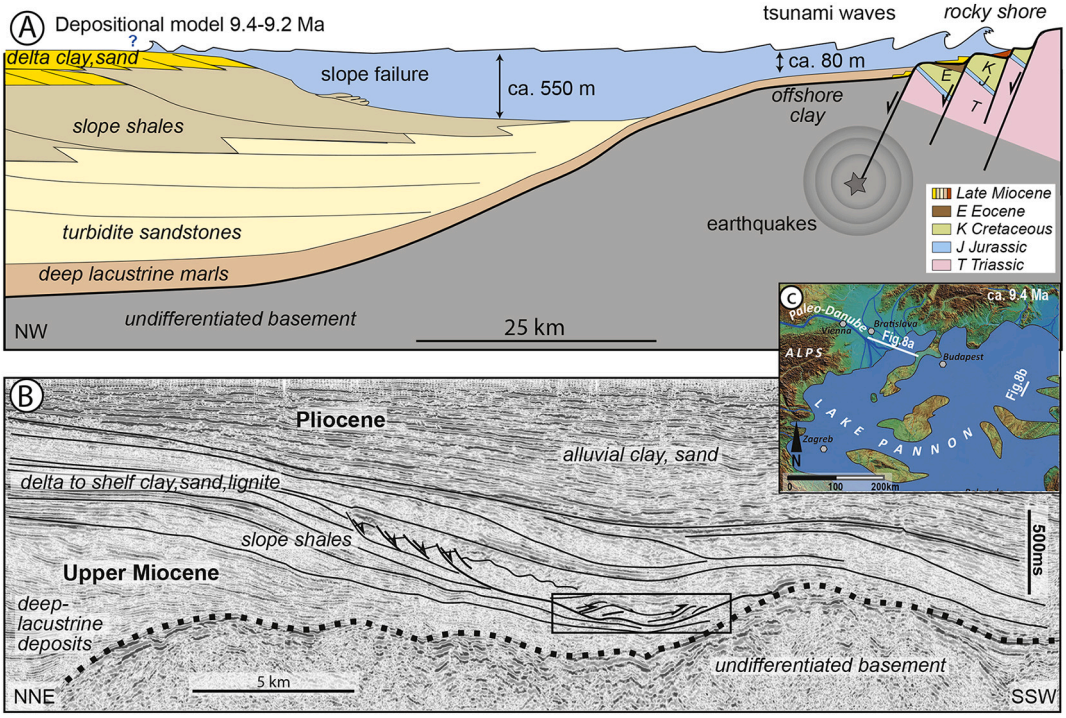

Fig. 8. A) Depositional model from the progradational slope of the deep lake to its fault-controlled margin, where the tsunami deposit formed due to earthquakes and/or slope failures as possible triggering mechanisms. B) Shelf progradation with large-scale slope failure shown on an interpreted seismic profile from the SE part of Lake Pannon. C) Location of the geological and seismic profiles.

4.6. Triggering mechanism

The triggering mechanism of a tsunami cannot be determined from the depositional features. Here we review some possible scenarios that could have caused tsunamis in Lake Pannon, without considering extra-terrestrial causes like the strike of a meteorite. A volcanic eruption, synsedimentary fault activity (paleoseismic event), and/or a major slide of the shelf-edge slope might have occurred anywhere in the vast Lake Pannon. A tsunami hitting the study area at the SE coast of the Kisalföld–Danube basin (Figs. 6, 8) must have been triggered in the NW part of the lake. At this time the length of the embayment was almost 200 km, its width was ca. 50 km and the depth attained 550 m in its central part (Sztanó et al., 2016; Balázs et al., 2018).

There are two major buried volcanoes in the Kisalföld–Danube basin: one in the central part and another at the northeastern margin. Their activity, however, which started in the middle Miocene and persisted to the late Miocene, came to an end at 11 Ma (Harangi et al., 1995; Harangi et al., 2015; Pánisová et al., 2018), i.e. some 2 million years before the studied tsunamiite was deposited.

Near-site structural observations provide good candidates for a triggering mechanism. Earthquakes might have been related to structural activity close to the site during the deposition of the gravel. This activity is manifested by several N-S trending fault segments in the study area (Fig. 1c), where fault-related breccias, large footwall-detached blocks, and abrasional gravels on eroded fault scarps indicate coeval faulting (Fig. 2; Fodor et al., 2018). In addition to local structural activity, any syn-sedimentary fault movement in the western part of the lake basin could have produced earthquakes, or the associated rock-fall could have been capable of triggering tsunami waves, potentially large enough to generate the documented tsunami deposit (Fig. 8). Although a far-field tsunami trigger would be more difficult to prove, evidence of active late Miocene faults, possibly not long before the deposition of the tsunamiite, are extensively documented not only from the Trandanubian Range, but all over the western Pannonian Basin (Kiss et al., 2001; Fodor, 2008; Törő et al., 2012; Fodor et al., 2013; Kovács et al., 2015; Vojtko et al., 2019).

Another source of tsunami events could have been the shelf edge slope of Lake Pannon, which was located ca. 50–80 km to the NW from the coast of the large Transdanubian peninsula when the gravel deposited (Fig. 8; Sztanó et al., 2016; Magyar et al., 2017). Close to the shelf-margin the water depth of Lake Pannon reached 550 m (calculated from decompacted clinoform height; Balázs et al., 2018), but it was only about 80 m in a 10–15 km wide belt near the coast of the study site (estimated from paleobiological data; Cziczer et al., 2009). As a consequence of high sediment input from the W-NW, an unusually rapid slope progradation occurred (ca. 100 km/Ma; cf. Magyar et al., 2013), probably inducing instable conditions. Therefore, the slope must have been especially prone to major slide events (Fig. 8b) due to autocyclic oversteepening even without earthquake shocking. Modest earthquakes, on the other hand, can initiate liquefaction in rapidly prograding delta and slope systems leading to failure and triggering tsunamis more commonly than formerly anticipated (Hornbach et al., 2010). If a subaqueous slope failure occurred somewhere along the ca. 150 km wide strike of the slope, it could have mobilized a large volume of sediment and thus could have very well initiated tsunami waves in Lake Pannon.

No such slope failure has been documented so far in the old-vintage 2D seismic data of the Kisalföld–Danube Basin. The progradation of the shelf edge slope, however, continued until 4 Ma over the entire area of the Pannonian basin (Magyar et al., 2013), and many examples of slope collapse events are detected in various 3D seismic volumes (Fig. 8; van Baak et al., 2017; Csicsák et al., 2018). These events must have been quite common in the sedimentary system of Lake Pannon, therefore tsunami events could have been equally frequent.

If tsunamis could have been so common in Lake Pannon, why have there not been more tsunami deposits detected along the paleoshorelines? Potential sand beds in delta plain deposits are numerous and are not peculiar. As discussed above, fine-grained tsunami deposits have a low preservation potential due to subsequent change of the paleoenvironment, erosion, bio- and pedoturbation, etc. (Spiske et al.,

2020). As tsunamis do not necessarily leave a large signal in the rock record, many of them remain unrecognized (Fig. 8a). Special conditions may be needed to amplify tsunami waves in order to exceed a threshold for producing noticeable deposits, which varies with coastal settings. The known paleogeographic conditions of the Kisalföld–Danube Basin might have played a role in the amplification of tsunami waves. If triggering occurred far to the south, the dimensions of the elongate, funnel-shaped embayment of the lake (Fig. 6e) could have resulted in resonant amplification of the wave motions (cf. Sztanó and de Boer, 1995). If more proximal triggering locations are considered, an otherwise small tsunami wave could have been amplified while propagating across the wide, relatively shallow-water "plateau" near the studied coast, resulting in a catastrophic flood of the coast and the accumulation of the studied tsunami deposit. Elsewhere, without local amplification, the erosional or depositional effect of the same tsunami could have remained unnoticed. The primary or refracted origin of the subsequent waves cannot be determined from the deposit. Both the likely steep shores from NE and the well-known progradational slope to N-NW (Fig. 6.e) could have reflected the tsunami wave as a topographic barrier.

The generally low preservation potential of backshore paleo-tsunami deposits (Paris et al., 2017; Pérez-Torrado et al., 2006) also impedes their recognition in the rock record. In our case, the continued flooding of the peninsula (Sztanó et al., 2016; Magyar et al., 2017), and burial of the succession resulted in its preservation. In addition, abrasional, nearshore or deltaic deposits which may interfinger with other potential paleo-tsunami deposits are cropping out only in narrow belts along the present hills (e.g. Magyar et al., 2017) and each exposure represents only a very limited time window. Therefore, up to date, this is the only study reporting tsunami deposits from the late Miocene of Lake Pannon.

5. Conclusions

There is no distinct facies model for fine- or coarse-grained onshore tsunamiites, because these can greatly vary depending on several local features. In addition, the sedimentary character of onshore gravels deposited from extreme wave events, i.e. tsunamis and storms can be similar. Only a thorough analysis may reveal a combination of features determined by transport and depositional processes that facilitate the identification of paleo-tsunami deposits.

In the case of the upper Miocene bouldery cobble gravel from the coast of Lake Pannon, various degrees of clast roundness, lakeward dipping imbrication, bidirectional transport indicators, clast-supported fabric, large bed thickness or lack of grading do not provide exclusive evidence in favor of either tsunami or storm wave origin. Extreme storm waves, however, are discarded considering the local paleogeography (with restricted width of the water body) and climate (with probably low-speed winds only). A combination of depositional signatures, e.g. the matrix-supported fabric and the preservation of the articulated mollusc shells, as well as mixture of clasts and fossils from different coastal zones offshore to backshore, favor the classification of these beds as paleo-tsunami deposits.

Well-developed clast imbrication in the matrix-supported gravel reveals inundation of the backshore region by the first wave, followed by back wash and deposition of small sand dunes in erosional scours. The overlying imbricated, clast-supported gravel probably was formed by another successive tsunami wave, most likely from the same event. Tsunamiites do not reflect tsunami triggering mechanism. Faults that might have been active at times of deposition occur close to the study site. In addition, rapid slope progradation in Lake Pannon, or earthquakes related to the above faults may have resulted in slope collapse events triggering the tsunami.

Our interpretation confirms that coarse-grained onshore tsunami deposits, scarcely recognized in the rock record, may have formed in lacustrine settings. Fine-grained ones could have remained undiscovered, probably because physical conditions for amplification of tsunami waves were not met, or due to their low preservation potential. Lacustrine tsunami deposits may be more abundant than previously thought, if contemporary structural deformation, volcanism, or the collapse of steep slopes due to high sedimentation rates are considered. Finally, it is concluded that tsunami deposits in the deep time rock record, particularly in continental settings, may serve as indicators of paleoseismicity and may help to identify otherwise unknown structural activity in the area. Both lacustrine and marine paleo-tsunamiites can highlight specific paleogeographic configurations favorable for amplification of tsunami waves.

Declaration of Competing Interest

The authors declare that they have no known competing financial interests or personal relationships that could have appeared to influence the work reported in this paper.

Acknowledgements

We dedicate this study to our late mentor and friend Frank Horváth, who showed us how the small-scale pieces of evidence from various parts of geology fit together in order to understand the large-scale formation and evolution of sedimentary basins. Field assistance by Zoltán Lantos (MBFSZ) and Szilvia Kövér (MTA-ELTE), determination of ostracods by Vivien Csoma (ELTE) is appreciated. We are grateful to Poppe de Boer, Whitney Autin, Paul Myers and Pedro Costa for excellent suggestions and critical remarks on a previous version of the manuscript. Our special thanks go to Arnoud Slootman for further thought-provoking comments and linguistic advises that improved greatly the overall clarity of the paper. This research was supported by the Hungarian National Research, Development and Innovation Office (NKFI) projects no. 81530 and 116618. This is MTA-MTM-ELTE Paleo contribution No. 327.

References

Abad, M., Izquierdo, T., Cáceres, M., Bernárdez, E., Rodriguez-Vidal, J., 2020. Coastal boulder deposit as evidence of an ocean-wide prehistoric tsunami originated on the Atacama Desert coast (northern Chile). Sedimentology 67, 1505–1528. https://doi.org/10.1111/sed.12570.

Bahlburg, H., Spiske, M., Weiss, R., 2010. Comment on " Sedimentary features of tsunami backwash deposits in a shallow marine Miocene setting, Mejillones Peninsula, northern Chile " by G. Cantalamessa and C. Di Celma. Sediment. Geol. 228, 77–80. https://doi.org/10.1016/j.sedgeo.2010.03.006.

Bahlburg, H., Nentwig, H., Kreutzer, M., 2018. The September 16, 2015 Illapel tsunami, Chile – Sedimentology of tsunami deposits at the beaches of La Serena and Coquimbo. Mar. Geol. 396, 43–53. https://doi.org/10.1016/j.margeo.2016.12.011.

Balázs, A., Matenco, L., Magyar, I., Horváth, F., Cloetingh, S., 2016. The link between tectonics and sedimentation in back-arc basins: New genetic constraints from the analysis of the Pannonian Basin. Tectonics 35, 1526–1559. https://doi.org/10.1002/2015TC004109.

Balázs, A., Burov, E., Matenco, L., Vogt, K., Francois, T., Cloetingh, S., 2017a. Symmetry during the syn- and post-rift evolution of extensional back-arc basins: the role of inherited orogenic structures. Earth Planet. Sci. Lett. 462, 86–98. https://doi.org/10.1016/j.epsl.2017.01.015.

Balázs, A., Granjeon, D., Matenco, L., Sztanó, O., Cloetingh, S., 2017b. Tectonic and climatic controls on asymmetric half-graben sedimentation: inferences from 3D numerical modeling. Tectonics 36, 2123–2141. https://doi.org/10.1002/2017TC004647.

Balázs, A., Magyar, I., Matenco, L., Sztanó, O., Tőkés, L., Horváth, F., 2018. Morphology of a large paleo-lake: analysis of compaction in the Miocene-Quaternary Pannonian Basin. Glob. Planet. Chang. 171, 134–147. https://doi.org/10.1016/j.gloplacha.2017.10.012.

Bartha, I., Magyar, I., Fodor, L., Csillag, G., Lantos, Z., Tőkés, L., Sztanó, O., 2015. Lake Pannon Deltaic deposits in Gerecse hills, Hungary. In: Abstract Book of 31st IAS meeting of Sedimentology: International Association of Sedimentologists, pp. 54.

Bartholy, J., Radics, K., Bohoczky, F., 2003. Present state of wind energy utilisation in Hungary: Policy, wind climate, and modelling studies. Renew. Sust. Energ. Rev. 7, 175–186. https://doi.org/10.1016/S1364-0321(03)00003-0.

Böhme, M., Ilg, A., Winklhofer, M., 2008. Late Miocene "washhouse" climate in Europe. Earth Planet. Sci. Lett. 275, 393–401. https://doi.org/10.1016/j.epsl.2008.09.011.

Bondevik, S., Svendsen, J.I., Mangerud, J., 1997. Tsunami sedimentary facies deposited by the Storegga tsunami in shallow marine basins and coastal lakes, western Norway.

Sedimentology 44, 1115–1131. https://doi.org/10.1046/j.1365-3091.1997.d01-63.x.
Bourgeois, J., Hansen, A.T., Wilberg, L.P., Kauffman, G.E., 1988. A Tsunami deposit at the cretaceous-tertiary boundary in Texas. Science 241, 567–570. https://doi.org/10.1126/science.241.4865.567.
Cantalamessa, G., Di Celma, C., 2005. Sedimentary features of tsunami backwash deposits in a shallow marine Miocene setting, Mejillones Peninsula, northern Chile. Sediment. Geol. 178, 259–273. https://doi.org/10.1016/j.sedgeo.2005.05.007.
Chagué-Goff, C., Schneider, J.-L., Goff, J.R., Dominey-Howes, D., Strotz, L., 2011. Expanding the proxy toolkit to help identify past events — Lessons from the 2004 Indian Ocean Tsunami and the 2009 South Pacific Tsunami. Earth-Sci. Rev. 107, 107–122. https://doi.org/10.1016/j.earscirev.2011.03.007.
Costa, P.J.M., Andrade, C., 2020. Tsunami deposits: present knowledge and future challenges. Sedimentology 1189–1206. https://doi.org/10.1111/sed.12724.
Costa, P.J.M., Andrade, C., Freitas, M.C., Oliveira, M.A., da Silva, C.M., Omira, R., Taborda, R., Baptista, M.A., Dawson, A.G., 2011. Boulder deposition during major tsunami events. Earth Surf. Process. Landf. 36, 2054–2068. https://doi.org/10.1002/esp.2228.
Costa, P.J.M., Leroy, S.A.G., Dinis, J.L., Dawson, A.G., Kortekaas, S., 2012. Recent high-energy marine events in the sediments of Lagoa de Óbidos and Martinhal (Portugal): recognition, age and likely causes. Nat. Hazards Earth Syst. Sci. 12, 1367–1380. https://doi.org/10.5194/nhess-12-1367-2012.
Cox, R., Zentner, D.B., Kirchner, B.J., Cook, M.S., 2012. Boulder Ridges on the Aran Islands (Ireland): recent movements caused by storm waves, not tsunamis. J. Geol. 120, 249–272. https://doi.org/10.1086/664787.
Cox, R., Jahn, K.L., Watkins, O.G., Cox, P., 2018. Extraordinary boulder transport by storm waves (west of Ireland, winter 2013–2014), and criteria for analysing coastal boulder deposits. Earth-Sci. Rev. 177, 623–636. https://doi.org/10.1016/j.earscirev.2017.12.014.
Csicsák, P., Márton, B., Sztanó, O., 2018. Shelf collapse, tilting and hydrocarbon trap formation on deltaic to slope deposits (Újfalu and Algyő Formations), Battonya-high, late Miocene Pannonian Basin. In: Abstract Book of XXI International congress of the CBGA, Salzburg, Austria, pp. 325.
Csontos, L., 1995. Tertiary tectonic evolution of the Intra-Carpathian area: a review. Acta Vulcanol. 7, 1–13.
Cziczer, I., Magyar, I., Pipík, R., Böhme, M., Ćorić, S., Bakrač, K., Sütő-Szentai, M., Lantos, M., Babinszki, E., Müller, P., 2009. Life in the sublittoral zone of long-lived Lake Pannon: paleontological analysis of the Upper Miocene Szák Formation, Hungary. Int. J. Earth Sci. 98, 1741–1766. https://doi.org/10.1007/s00531-008-0322-3.
Davies, I.C., Walker, R.G., 1974. Transport and deposition of resedimented conglomerates; the Cap Enrage Formation, Cambro-Ordovician, Gaspe, Quebec. J. Sediment. Res. 44, 1200–1216. https://doi.org/10.1306/212f6c76-2b24-11d7-8648000102c1865d.
Davies, D.J., Powell, E.N., Stanton, R.J., 1989. Taphonomic signature as a function of environmental process: Shells and shell beds in a hurricane-influenced inlet on the Texas coast. Palaeogeogr. Palaeoclimatol. Palaeoecol. 72, 317–356. https://doi.org/10.1016/0031-0182(89)90150-8.
Dawson, A.G., 1994. Geomorphological effects of tsunami run-up and backwash. Geomorphology 10, 83–94. https://doi.org/10.1016/0169-555x(94)90009-4.
Dawson, A.G., Stewart, I., 2007. Tsunami deposits in the geological record. Sediment. Geol. 200, 166–183. https://doi.org/10.1016/j.sedgeo.2007.01.002.
Dawson, A.G., Lockett, P., Shi, S., 2004. Tsunami hazards in Europe. Environ. Int. 30, 577–585. https://doi.org/10.1016/j.envint.2003.10.005.
Dawson, A.G., Dawson, S., Bondevik, S., Costa, P.J.M., Hill, J., Stewart, I., 2019. Reconciling Storegga tsunami sedimentation patterns with modelled wave heights: a discussion from the Shetland Isles field laboratory. Sedimentology 1344–1353. https://doi.org/10.1111/sed.12643.
Dewey, J.F., Ryan, P.D., 2017. Storm, rogue wave, or tsunami origin for megaclast deposits in western Ireland and North Island, New Zealand? Proc. Natl. Acad. Sci. U. S. A. 114, E10639–E10647. https://doi.org/10.1073/pnas.1713233114.
Donato, S.V., Reinhardt, E.G., Boyce, J.I., Rothaus, R., Vosmer, T., 2008. Identifying tsunami deposits using bivalve shell taphonomy. Geology 36, 199–202. https://doi.org/10.1130/G24554A.1.
Erdmann, W., Kelletat, D., Kuckuck, M., 2017. Boulder Ridges and Washover Features in Galway Bay, Western Ireland. J. Coast. Res. 335, 997–1021. https://doi.org/10.2112/jcoastres-d-16-00184.1.
Etienne, S., Paris, R., 2010. Boulder accumulations related to storms on the south coast of the Reykjanes Peninsula (Iceland). Geomorphology 114, 55–70. https://doi.org/10.1016/j.geomorph.2009.02.008.
Etienne, S., Buckley, M., Paris, R., Nandasena, A.K., Clark, K., Strotz, L., Chagué-Goff, C., Goff, J., Richmond, B., 2011. The use of boulders for characterising past tsunamis: Lessons from the 2004 Indian Ocean and 2009 South Pacific tsunamis. Earth-Sci. Rev. 107, 76–90. https://doi.org/10.1016/j.earscirev.2010.12.006.
Falvard, S., Paris, R., Belousova, M., Belousov, A., Giachetti, T., Cuven, S., 2018. Scenario of the 1996 volcanic tsunamis in Karymskoye Lake, Kamchatka, inferred from X-ray tomography of heavy minerals in tsunami deposits. Mar. Geol. 396, 160–170. https://doi.org/10.1016/j.margeo.2017.04.011.
Felton, E.A., Crook, K.A.W., Keating, B.H., Kay, E.A., 2006. Sedimentology of rocky shorelines: 4. Coarse gravel lithofacies, molluscan biofacies, and the stratigraphic and eustatic records in the type area of the Pleistocene Hulopoe Gravel, Lanai, Hawaii. Sediment. Geol. 184, 1–76. https://doi.org/10.1016/j.sedgeo.2005.08.005.
Fodor, L., 2008. Structural geology. In: Budai, T., Fodor, L. (Eds.), Geology of the Vértes Hills. Explanatory Book to the Geological Map of the Vértes Hills 1:50000. 145-202. Hungarian Geological Institute, pp. 282–300.
Fodor, L., Csontos, L., Magyar, I., Törő, B., Uhrin, A., Várkonyi, A., Csillag, G., Kövér, Sz., Lantos, Z., Tőkés, L., 2013. Late Miocene depositional units and syn-sedimentary deformation in the western Pannonian basin, Hungary. In: Abstract Book of 11th Workshop on Alpine Geological Studies, 7th European Symposium on Fossil Algae. Abstracts, Field Guides. Schladming, 8–14th September 2013. Berichte Der Geologischen Bundesanstalt, Schladming, pp. 33–34.
Fodor, L., Kercsmár, Z., Kövér, Sz., 2018. Structure and deformation phases of the Gerecse. In: Budai, T. (Ed.), Geology of the Gerecse Mountains. Mining and Geological Survey of Hungary, Budapest, pp. 169–208 (370–386).
Fujino, S., Masuda, F., Tagamori, S., Matsumoto, D., 2006. Structure and depositional processes of a gravelly tsunami deposit in a shallow marine setting: lower cretaceous Miyako Group, Japan. Sediment. Geol. 187, 127–138. https://doi.org/10.1016/j.sedgeo.2005.12.021.
Gelfenbaum, G., Jaffe, B., 2003. Erosion and sedimentation from the 17 July, 1998 Papua New Guinea Tsunami. Pure Appl. Geophys. 160, 1969–1999. https://doi.org/10.1007/s00024-003-2416-y.
Gillet, S., Marinescu, F., 1971. La faune malacologique pontienne de Rădmăneşti (Banat Roumain). Institut. Géologique, Mémoires 15, 1–78.
Goff, J., Chagué-Goff, C., Nichol, S., 2001. Palaeotsunami deposits: a New Zealand perspective. Sediment. Geol. 143, 1–6. https://doi.org/10.1016/s0037-0738(01)00121-x.
Goff, J., Chagué-Goff, C., Nichol, S., Jaffe, B., Dominey-Howes, D., 2012. Progress in palaeotsunami research. Sediment. Geol. 243–244, 70–88. https://doi.org/10.1016/j.sedgeo.2011.11.002.
Goto, K., Chagué-Goff, C., Goff, J., Jaffe, B., 2012. The future of tsunami research following the 2011 Tohoku-oki event. Sedimentary Geology 282, 1–13. https://doi.org/10.1016/j.sedgeo.2012.08.003.
Goto, K., Ikehara, K., Goff, J., Chagué-Goff, C., Jaffe, B., 2014. The 2011 Tohoku-oki tsunami - three years on. Mar. Geol. 358, 2–11. https://doi.org/10.1016/j.margeo.2014.08.008.
Goto, T., Satake, K., Sugai, T., Ishibe, T., Harada, T., Murotani, S., 2015. Historical tsunami and storm deposits during the last five centuries on the Sanriku coast. Japan. Mar. Geol. 367, 105–117. https://doi.org/10.1016/j.margeo.2015.05.009.
Goto, T., Satake, K., Sugai, T., Ishibe, T., Harada, T., Gusman, A.R., 2019. Tsunami history over the past 2000 years on the Sanriku coast, Japan, determined using gravel deposits to estimate tsunami inundation behavior. Sediment. Geol. 382, 85–102. https://doi.org/10.1016/j.sedgeo.2019.01.001.
Hably, L., 2013. The late Miocene flora of Hungary. Geol. Hung. Ser. Palaeontol. 56, 175.
Hall, A.M., Hansom, J.D., Williams, D.M., Jarvis, J., 2006. Distribution, geomorphology and lithofacies of cliff-top storm deposits: examples from the high-energy coasts of Scotland and Ireland. Mar. Geol. 232, 131–155. https://doi.org/10.1016/j.margeo.2006.06.008.
Harangi, Sz., Lenkey, L., 2007. Genesis of the Neogene to Quaternary volcanism in the Carpathian-Pannonian region: Role of subduction, extension, and mantle plume. Geol. Soc. Am. Spec. Pap. 418, 67–92. https://doi.org/10.1130/2007.2418(04).
Harangi, Sz., Vaselli, O., Tonarini, S., Szabó, Cs., Harangi, R., Coradossi, N., 1995. Petrogenesis of Neogene extension-related alkaline volcanic rocks of the Little Hungarian Plain Volcanic field (Western Hungary). Acta Vulcanol. 7, 173–187.
Harangi, Sz., Jankovics, M.É., Sági, T., Kiss, B., Lukács, R., Soós, I., 2015. Origin and geodynamic relationship of the Late Miocene to Quaternary alkaline basalt volcanism in the Pannonian basin, eastern-central Europe. Int. J. Earth Sci. 104, 2007–2032. https://doi.org/10.1007/s00531-014-1105-7.
Harzhauser, M., Mandic, O., 2010. Neogene dreissenids in Central Europe: Evolutionary shifts and diversity changes. In: Van der Velde, G., Rajagopal, S., Bij de Vaate, A. (Eds.), The Zebra Mussel in Europe. Backhuys Publishers, Leiden, Margraf Publishers, Weikersheim, pp. 490.
Hayes, M.O., Michel, J., Betenbaugh, D.V., 2010. The Intermittently exposed, coarse-grained gravel beaches of prince William Sound, Alaska: comparison with open-ocean gravel beaches. J. Coast. Res. 261, 4–30. https://doi.org/10.2112/08-1071.
Hilbe, M., Anselmetti, F.S., 2014. Signatures of slope failures and river-delta collapses in a perialpine lake (Lake Lucerne, Switzerland). Sedimentology 61, 1883–1907. https://doi.org/10.1111/sed.12120.
Hoffmeister, D., Curdt, C., Bareth, G., 2020. Monitoring the sedimentary budget and dislocated boulders in western Greece – results since 2008. Sedimentology 67, 1411–1430. https://doi.org/10.1111/sed.12723.
Hornbach, M.J., Braudy, N., Briggs, R.W., Cormier, M., Davis, M.B., Diebold, J.B., Dieudonne, N., Douilly, R., Frohlich, C., Gulick, S.P.S., Johnson III, H.E., Mann, P., McHugh, C., Ryan-Mishkin, K., Prentice, C.S., Seeber, L., Sorlien, C.C., Steckler, M.S., Symithe, S.J., Taylor, F.W., Templeton, J., 2010. High tsunami frequency as a result of combined strike-slip faulting and coastal landslides. Nat. Geosci. 3, 783–788. https://doi.org/10.1038/ngeo975.
Ichinose, G.A., Anderson, J.G., Satake, K., Schweickert, R.A., Lahren, M.M., 2000. The potential hazard from tsunami and seiche waves generated by large earthquakes within Lake Tahoe, California-Nevada. Geophys. Res. Lett. 27, 1203–1206. https://doi.org/10.1029/1999gl011119.
Jarochowska, E., Munnecke, A., 2015. Silurian carbonate high-energy deposits of potential tsunami origin: Distinguishing lateral redeposition and time averaging using carbon isotope chemostratigraphy. Sediment. Geol. 315, 14–28. https://doi.org/10.1016/j.sedgeo.2014.10.012.
Kempf, P., Moernaut, J., Van Daele, M., Vandoorne, W., Pino, M., Urrutia, R., De Batist, M., 2017. Coastal lake sediments reveal 5500 years of tsunami history in south Central Chile. Quat. Sci. Rev. 161, 99–116. https://doi.org/10.1016/j.quascirev.2017.02.018.
Kiss, A., Gellért, B., Fodor, L., 2001. Structural history of the Porva Basin in the Northern Bakony Mts. (Western Hungary): Implications for the Mesozoic and Tertiary tectonic evolution of the Transdanubian Range and Pannonian Basin. Geol. Carpath. 52, 183–190.
Kortekaas, S., Dawson, A.G., 2007. Distinguishing tsunami and storm deposits: an

example from Martinhal, SW Portugal. Sediment. Geol. 200, 208–221. https://doi.org/10.1016/j.sedgeo.2007.01.004.
Kováč, M., Baráth, I., Fordinál, K., Grigorovich, A.S., Halásová, E., Hudáčková, N., Joniak, P., Sabol, M., Slamková, M., Sliva, Ľ., Vojtko, R., 2006. Late Miocene to early Pliocene sedimentary environments and climatic changes in the Alpine-Carpathian-Pannonian junction area: a case study from the Danube Basin northern margin (Slovakia). Palaeogeogr. Palaeoclimatol. Palaeoecol. 238, 32–52. https://doi.org/10.1016/j.palaeo.2006.03.015.
Kovács, G., Fodor, L., Kövér, Sz., Molnár, G., Raáb, D., Telbisz, T., Timár, G., 2015. Verification of Late Miocene to Quaternary structural control on landforms: a case study with comprehensive methodology from a low hilly area (western Pannonian Basin). Austrian J. Earth Sci. 108 (2), 82–104. https://doi.org/10.17738/ajes.2015.0015.
Kovar-Eder, J., Hably, L., 2006. The flora of Mataschen – a unique plant assemblage from the late Miocene of Eastern Styria (Austria). Acta Palaeobotanica 46 (2), 157–239.
Kremer, K., Hilbe, M., Simpson, G., Decrouy, L., Wildi, W., Girardclos, S., 2015. Reconstructing 4000 years of mass movement and tsunami history in a deep peri-Alpine lake (Lake Geneva, France-Switzerland). Sedimentology 62, 1305–1327. https://doi.org/10.1111/sed.12190.
Lario, J., Spencer, C., Bardají, T., Marchante, Á., Garduño-monroy, V.H., Macias, J., Ortega, S., 2020. An extreme wave event in eastern Yucatán, Mexico: Evidence of a palaeotsunami event during the Mayan times. Sedimentology. https://doi.org/10.1111/sed.12662.
Lukács, R., Harangi, Sz., Guillong, M., Bachman, O., Fodor, L., Buret, Y., Dunkl, I., Sliwinski, J., von Quadt, A., Peytcheva, I., Zimmerer, M., 2018. Early to Mid-Miocene syn-extensional massive silicic volcanism in the Pannonian Basin (East-Central Europe): Eruption chronology, correlation potential and geodynamic implications. Earth-Sci. Rev. 179, 1–19. https://doi.org/10.1016/j.earscirev.2018.02.005.
Magyar, I., 2020. Chronostratigraphy of Clinothem-Filled Non-Marine Basins: Dating the Pannonian Stage. this volume.
Magyar, I., Geary, D.H., Müller, P., 1999. Paleogeographic evolution of the late Miocene Lake Pannon in Central Europe. Palaeogeogr. Palaeoclimatol. Palaeoecol. 147, 151–167. https://doi.org/10.1016/s0031-0182(98)00155-2.
Magyar, I., Radivojević, D., Sztanó, O., Synak, R., Ujszászi, K., Pócsik, M., 2013. Progradation of the paleo-Danube shelf margin across the Pannonian Basin during the Late Miocene and Early Pliocene. Glob. Planet. Chang. 103, 168–173. https://doi.org/10.1016/j.gloplacha.2012.06.007.
Magyar, I., Sztanó, O., Csillag, G., Kercsmár, Z., Katona, L., Lantos, Z., Bartha, I.R., Fodor, L., 2017. Pannonian molluscs and their localities in the Gerecse Hills, Transdanubian Range : stratigraphy, palaeoenvironment, geological evolution. Földtani Közlöny 147, 149–176. https://doi.org/10.23928/foldt.kozl.2017.147.2.149.
Major, J.J., 1998. Pebble orientation on large, experimental debris-flow deposits. Sediment. Geol. 117, 151–164. https://doi.org/10.1016/S0037-0738(98)00014-1.
Maouche, S., Morhange, C., Meghraoui, M., 2009. Large boulder accumulation on the Algerian coast evidence tsunami events in the western Mediterranean. Mar. Geol. 262, 96–104. https://doi.org/10.1016/j.margeo.2009.03.013.
Marinescu, Fl, 1977. Genre *Dreissenomya* Fuchs (Bivalvia, Heterodonta). Institut de Géologie et de Géophysique, Mémoires 26, 75–118.
Massari, F., D'Alessandro, A., Davaud, E., 2009. A coquinoid tsunamite from the Pliocene of Salento (SE Italy). Sediment. Geol. 221 (1-4), 7–18. https://doi.org/10.1016/j.sedgeo.2009.07.007.
Massari, F., Parea, G., 1988. Progradational gravel beach sequences in a moderate- to high-energy, microtidal marine environment. Sedimentology 35, 881–913. https://doi.org/10.1111/j.1365-3091.1988.tb01737.x.
Mastronuzzi, G., Pignatelli, C., Sansò, P., Selleri, G., 2007. Boulder accumulations produced by the 20th of February, 1743 tsunami along the coast of southeastern Salento (Apulia region, Italy). Mar. Geol. 242, 191–205. https://doi.org/10.1016/j.margeo.2006.10.025.
Matsumoto, D., Shimamoto, T., Hirose, T., Gunatilake, J., Wickramasooriya, A., DeLile, J., Young, S., Rathnayake, C., Ranasooriya, J., Murayama, M., 2010. Thickness and grain-size distribution of the 2004 Indian Ocean tsunami deposits in Periya Kalapuwa Lagoon, eastern Sri Lanka. Sediment. Geol. 230, 95–104. https://doi.org/10.1016/j.sedgeo.2010.06.021.
Moore, A.L., 2000. Landward fining in onshore gravel as evidence for a late Pleistocene tsunami on Molokai, Hawaii. Geology 28, 247–250. https://doi.org/10.1130/0091-7613(2000)028<0247:lfioga>2.3.co;2.
Moore, J.G., Moore, G.W., 1984. Deposit from a giant wave on the Island of Lanai, Hawaii. Science 226, 1312–1315. https://doi.org/10.1126/science.226.4680.1312.
Moore, J.G., Bryan, W.B., Ludwig, K.R., 1994. Chaotic deposition by a giant wave, Molokai, Hawaii. Geol. Soc. Am. Bull. 106, 962–967. https://doi.org/10.1130/0016-7606(1994)106<0962:cdbagw>2.3.co;2.
Morton, R.A., Gelfenbaum, G., Jaffe, B.E., 2007. Physical criteria for distinguishing sandy tsunami and storm deposits using modern examples. Sediment. Geol. 200, 184–207. https://doi.org/10.1016/j.sedgeo.2007.01.003.
Morton, R.A., Richmond, B.M., Jaffe, B.E., Gelfenbaum, G., 2008. Coarse-Clast Ridge complexes of the Caribbean: a preliminary basis for distinguishing Tsunami and storm-wave origins. J. Sediment. Res. 78, 624–637. https://doi.org/10.2110/jsr.2008.068.
Mulder, T., Alexander, J., 2001. The physical character of subaqueous sedimentary density flow and their deposits. Sedimentology 48, 269–299. https://doi.org/10.1046/j.1365-3091.2001.00360.x.
Nagy, E., 2005. Palynological evidence for Neogene climatic change in Hungary. In: Occasional Papers of the Geological Institute of Hungary. 205. pp. 120.
Nanayama, F., 2008. Sedimentary Characteristics and Depositional Processes of Onshore Tsunami deposits: An example of Sedimentation Associated with the 12 July 1993 Hokkaido–Nansei-oki Earthquake Tsunami. In: Shiki, T., Tsuji, Y., Minoura, K., Yamazaki, T. (Eds.), Tsunamiites - Features and Implications. Elsevier, Oxford, pp. 63–80. https://doi.org/10.1016/b978-0-444-51552-0.00005-9.
Nanayama, F., Shigeno, K., 2006. Inflow and outflow facies from the 1993 tsunami in Southwest Hokkaido. Sediment. Geol. 187, 139–158. https://doi.org/10.1016/j.sedgeo.2005.12.024.
Nanayama, F., Shigeno, K., Satake, K., Shimokawa, K., Koitabashi, S., Miyasaka, S., 2000. Sedimentary differences between the 1993 Hokkaido-nansei-oki tsunami and the 1959 Miyakojima typhoon at Taisei, southwestern Hokkaido, northern Japan. Sediment. Geol. 135, 255–264. https://doi.org/10.1016/s0037-0738(00)00076-2.
Nargowalla, M.C., Hutchinson, M., Begun, D.R., 2006. Middle and late Miocene terrestrial vertebrate localities and paleoenvironments in the Pannonian Basin. Beitr. Paläontol. 30, 347–360.
Nemec, W., Steel, R.J., 1984. Alluvial and coastal conglomerates: their significant features and some comments on gravelly mass-flow deposits. In: Koster, E.H., Steel, R.J. (Eds.), Sedimentology of Gravels and Conglomerates. Mem. Can. Soc. Petrol. Geol. 10. pp. 1–31.
Olteanu, R., 2011. Atlas of the Pannonian and Pontian ostracods from the eastern area of the Pannonian Basin. Geo-Eco-Marina 17, 13–177.
Pánisová, J., Balázs, A., Zalai, Zs., Bielik, M., Horváth, F., Harangi, Sz., Schmidt, S., Götze, H.-J., 2018. Intraplate volcanism in the Danube Basin of NW Hungary: 3D geophysical modelling of the late Miocene Pásztori volcano. Int. J. Earth Sci. 107, 1713–1730. https://doi.org/10.1007/s00531-017-1567-5.
Paris, R., Giachetti, T., Chevalier, J., Guillou, H., Frank, N., 2011. Tsunami deposits in Santiago Island (Cape Verde archipelago) as possible evidence of a massive flank failure of Fogos volcano. Sediment. Geol. 239, 129–145. https://doi.org/10.1016/j.sedgeo.2011.06.006.
Paris, R., Kelfoun, K., Giachetti, T., 2013. Marine conglomerate and reef megaclasts at Mauritius Islands: Evidences of a tsunami generated by a flank collapse of the Piton de La Fournaise volcano, Reunion Island? Sci. Tsunami Hazards 32, 281–291.
Paris, R., Bravo, J.J.C., González, M.E.M., Kelfoun, K., Nauret, F., 2017. Explosive eruption, flank collapse and megatsunami at Tenerife ca. 170 ka. Nat. Commun. 8, 1–8. https://doi.org/10.1038/ncomms15246.
Paris, R., Ramalho, R.S., Madeira, J., Ávila, S., May, S.M., Rixhon, G., Engel, M., Brückner, H., Herzog, M., Schukraft, G., Perez-Torrado, F.J., Rodriguez-Gonzalez, A., Carracedo, J.C., Giachetti, T., 2018. Mega-tsunami conglomerates and flank collapses of ocean island volcanoes. Mar. Geol. 395, 168–187. https://doi.org/10.1016/j.margeo.2017.10.004.
Pérez-Torrado, F.J., Paris, R., Cabrera, M.C., Schneider, J.L., Wassmer, Carracedo, J.C., Rodríguez-Santana, Á., Santana, F., 2006. Tsunami deposits related to flank collapse in oceanic volcanoes: the Agaete Valley evidence, Gran Canaria, Canary Islands. Mar. Geol. 227, 135–149. https://doi.org/10.1016/j.margeo.2005.11.008.
Peters, R., Jaffe, B., Gelfenbaum, G., 2007. Distribution and sedimentary characteristics of tsunami deposits along the Cascadia margin of western North America. Sediment. Geol. 200, 372–386. https://doi.org/10.1016/j.sedgeo.2007.01.015.
Pilarczyk, J.E., Sawai, Y., Matsumoto, D., Namegaya, Y., Nishida, N., Ikehara, K., Fujiwara, O., Gouramanis, C., Dura, T., Horton, B., 2019. Constraining sediment provenance for tsunami deposits using distributions of grain size and foraminifera from the Kujukuri coastline and shelf, Japan. Sedimentology 67, 1373–1392. https://doi.org/10.1111/sed.12591.
Postma, G., Nemec, W., 1990. Regressive and transgressive sequences in a raised Holocene gravelly beach, southwestern Crete. Sedimentology 37, 907–920. https://doi.org/10.1111/j.1365-3091.1990.tb01833.x.
Puga-Bernabéu, Á., Aguirre, J., 2017. Contrasting storm- versus tsunami-related shell beds in shallow-water ramps. Palaeogeogr. Palaeoclimatol. Palaeoecol. 471, 1–14. https://doi.org/10.1016/j.palaeo.2017.01.033.
Richmond, B., Szczuciński, W., Chagué-Goff, C., Goto, K., Sugawara, D., Witter, R., Tappin, D.R., Jaffe, B., Fujino, S., Nishimura, Y., Goff, J., 2012. Erosion, deposition and landscape change on the Sendai coastal plain, Japan, resulting from the March 11, 2011 Tohoku-oki tsunami. Sediment. Geol. 282, 27–39. https://doi.org/10.1016/j.sedgeo.2012.08.005.
Royden, L.H., Horváth, F., 1988. The Pannonian basin. A Study in Basin Evolution. American Association of Petroleum Geologists. Memoir 45.
Scheffers, A., Scheffers, S., 2006. Documentation of the Impact of Hurricane Ivan on the Coastline of Bonaire (Netherlands Antilles). J. Coast. Res. 226, 1437–1450. https://doi.org/10.2112/05-0535.1.
Scheffers, A., Scheffers, S., Kelletat, D., 2005. Paleo-Tsunami relics on the Southern and Central Antillean Island Arc. J. Coast. Res. 212, 263–273. https://doi.org/10.2112/03-0144.1.
Scheffers, S.R., Haviser, J., Browne, T., Scheffers, A., 2009. Tsunamis, hurricanes, the demise of coral reefs and shifts in prehistoric human populations in the Caribbean. Quat. Int. 195, 69–87. https://doi.org/10.1016/j.quaint.2008.07.016.
Schnellmann, M., Anselmetti, F.S., Giardini, D., McKenzie, J.A., 2006. 15,000 years of mass-movement history in Lake Lucerne: Implications for seismic and tsunami hazards. Eclogae Geol. Helv. 99, 409–428. https://doi.org/10.1007/s00015-006-1196-7.
Scicchitano, G., Monaco, C., Tortorici, L., 2007. Large boulder deposits by tsunami waves along the Ionian coast of South-Eastern Sicily (Italy). Mar. Geol. 238, 75–91. https://doi.org/10.1016/j.margeo.2006.12.005.
Seghedi, I., Mațenco, L., Downes, H., Mason, R.D., Szakács, A., Pécskay, Z., 2011. Tectonic significance of changes in post-subduction Pliocene–Quaternary magmatism in the south east part of the Carpathian–Pannonian Region. Tectonophysics 502, 146–157. https://doi.org/10.1016/j.tecto.2009.12.003.
Shanmugam, G., 2012. Process-sedimentological challenges in distinguishing paleo-tsunami deposits. Nat. Hazards. 63, 5–30. https://doi.org/10.1007/s11069-011-9766-z.
Shiki, T., Yamazaki, T., 1996. Tsunami-induced conglomerates in Miocene upper bathyal deposits, Chita Peninsula, central Japan. Sediment. Geol. 104, 175–188. https://doi.

org/10.1016/0037-0738(95)00127-1.
Shiki, T., Yamazaki, T., 2008. The term “tsunamiite”. In: Shiki, T., Tsuji, Y., Yamazaki, T., Minoura, K. (Eds.), Tsunamiites - Features and Implications, pp. 5–7. https://doi.org/10.1016/b978-0-444-51552-0.00002-3.
Sipos-Benkő, K., Márton, E., Fodor, L., Pethe, M., 2014. An integrated magnetic susceptibility anisotropy (AMS) and structural geological study on Cenozoic clay-rich sediments from the Transdanubian Range. Cent. Eur. Geol. 57, 21–52. https://doi.org/10.1556/ceugeol.57.2014.1.2.
Slootman, A., Cartigny, M.J.B., Moscariello, A., Chiaradia, M., de Boer, L., 2016. Quantification of tsunami-induced flows on a Mediterranean carbonate ramp reveals catastrophic evolution. Earth Planet. Sci. Lett. 444, 192–204. https://doi.org/10.1016/j.epsl.2016.03.052.
Slootman, A., Simpson, G., Castelltort, S., de Boer, L., 2018. Geological record of marine tsunami-backwash: the role of the hydraulic jump. Depos. Rec. 1-19. https://doi.org/10.1002/dep2.38.
Spinoni, J., Szalai, S., Szentimrey, T., Lakatos, M., Bihari, Z., Nagy, A., Németh, Á., Kovács, T., Mihic, D., Dacic, M., Petrovic, P., Kržič, A., Hiebl, J., Auer, I., Milkovic, J., Štepánek, P., Zahradnícek, P., Kilar, P., Limanowka, D., Pyrc, R., Cheval, S., Birsan, M.V., Dumitrescu, A., Deak, G., Matei, M., Antolovic, I., Nejedlík, P., Štastný, P., Kajaba, P., Bochnícek, O., Galo, D., Mikulová, K., Nabyvanets, Y., Skrynyk, O., Krakovska, S., Gnatiuk, N., Tolasz, R., Antofie, T., Vogt, J., 2015. Climate of the Carpathian Region in the period 1961-2010: Climatologies and trends of 10 variables. Int. J. Climatol. 35, 1322–1341. https://doi.org/10.1002/joc.4059.
Spiske, M., Halley, R.B., 2014. A coral-rubble ridge as evidence for hurricane overwash, Anegada (British Virgin Islands). Adv. Geosci. 38, 9–20. https://doi.org/10.5194/adgeo-38-9-2014.
Spiske, M., Tang, H., Bahlburg, H., 2020. Post-depositional alteration of onshore tsunami deposits – Implications for the reconstruction of past events. Earth Sci. Rev. https://doi.org/10.1016/j.earscirev.2019.103068. In press.
Šujan, M., Braucher, R., Kováč, M., Bourlès, D.L., Rybár, S., Guillou, V., Hudáčková, N., 2016. Application of the authigenic 10Be/9Be dating method to late Miocene–Pliocene sequences in the northern Danube Basin (Pannonian Basin System): Confirmation of heterochronous evolution of sedimentary environments. Glob. Planet. Chang. 137, 35–53. https://doi.org/10.1016/j.gloplacha.2015.12.013.
Szilaj, R., Szónoky, M., Müller, Geary, D.H., Magyar, I., 1999. Stratigraphy, paleoecology, and paleogeography of the “*Congeria ungulacaprae* beds” (=*Lymnocardium ponticum* Zone) in NW Hungary: study of the Dáka outcrop. Acta Geol. Hung. 42, 33–55.
Sztanó, O., de Boer, P.L., 1995. Basin dimensions and morphology as controls on amplification of tidal motions (the Early Miocene North Hungarian Bay). Sedimentology 42 (4), 665–682. https://doi.org/10.1111/j.1365-3091.1995.tb00399.x.
Sztanó, O., Magyar, I., Szónoky, M., Lantos, M., Müller, Lenkey, L., Katona, L., Csillag, G., 2013a. Tihany Formation in the surroundings of Lake Balaton: type locality, depositional setting and stratigraphy. Földtani Közlöny 143, 73–98.
Sztanó, O., Szafián, P., Magyar, I., Horányi, A., Bada, G., Hughes, D.W., Hoyer, D.L., Wallis, R.J., 2013b. Aggradation and progradation controlled clinothems and deep-water sand delivery model in the Neogene Lake Pannon, Makó Trough, Pannonian Basin, SE Hungary. Glob. Planet. Chang. 103, 149–167. https://doi.org/10.1016/j.gloplacha.2012.05.026.
Sztanó, O., Kováč, M., Magyar, I., Šujan, M., Fodor, L., Uhrin, A., Rybár, S., Csillag, G., Tőkés, L., 2016. Late Miocene sedimentary record of the Danube/Kisalföld Basin: Interregional correlation of depositional systems, stratigraphy and structural evolution. Geol. Carpath. 67, 525–542. https://doi.org/10.1515/geoca-2016-0033.
Tanner, L.H., Calvari, S., 2004. Unusual sedimentary deposits on the SE side of Stromboli volcano, Italy: products of a tsunami caused by the ca. 5000 years BP Sciara del Fuoco collapse? J. Volcanol. Geotherm. Res. 137, 329–340. https://doi.org/10.1016/j.jvolgeores.2004.07.003.
Tari, G., 1994. Alpine Tectonics of the Pannonian Basin. PhD. Thesis. Rice University, Texas, USA (501 p).
Törő, B., Pratt, B.R., 2016. Sedimentary record of seismic events in the Eocene Green River Formation and its implications for regional tectonics on lake evolution (Bridger Basin, Wyoming). Sediment. Geol. 344, 175–204. https://doi.org/10.1016/j.sedgeo.2016.02.003.
Törő, B., Sztanó, O., Fodor, L., 2012. Inherited and syndepositional structural control on the evolution of Lake Pannon's slope, Northern Somogy, Hungary. Földtani Közlöny 142 (4), 339–356.
van Baak, C.G.C., Krijgsman, W., Magyar, I., Sztanó, O., Golovina, L.A., Grothe, A., Hoyle, T.M., Mandic, O., Patina, I.S., Popov, S., Radionova, E., Stoica, M., Vasiliev, I., 2017. Paratethys response to the Messinian salinity crisis. Earth-Sci. Rev. 172, 193–223. https://doi.org/10.1016/j.earscire2017.07.015.
Vasskog, K., Waldmann, N., Bondevik, S., Nesje, A., Chapron, E., Ariztegui, D., 2013. Evidence for Storegga tsunami run-up at the head of Nordfjord, western Norway. J. Quat. Sci. 28, 391–402. https://doi.org/10.1002/jqs.2633.
Vojtko, R., Klučiar, T., Králiková, S., Hók, J., Pelech, O., 2019. Late Badenian to Quaternary palaeostress evolution of the northeastern part of the Danube Basin and the southwestern slope of the Štiavnica Stratovolcano (Slovakia). Acta Geol. Slovaca 11, 15–29.
Wang, Y.-N., Zhang, M.-S., Li, X.-B., Yang, M., 2015. The sedimentary record of a Mesoproterozoic tsunami from the North China Craton. Geol. J. 50, 56–70. https://doi.org/10.1002/gj.
Williams, D.M., Hall, A.M., 2004. Cliff-top megaclast deposits of Ireland, a record of extreme waves in the North Atlantic—storms or tsunamis? Mar. Geol. 206, 101–117. https://doi.org/10.1016/j.margeo.2004.02.002.
Zingg, T., 1935. Beitrag zur Schotteranalyse. – Schweizeriscke Mineralogische und Petrologische Mitteilungen. 15. pp. 39–140.